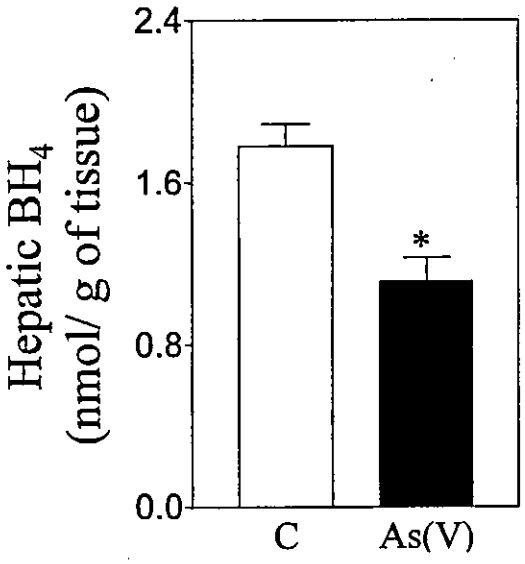

Fig. 5. Effects of prolonged arsenate exposure on the hepatic BH_4 levels. C = control; As(V) = arsenate. Each data point is the mean ± SD of six animals. * $p < .05$ vs. control.

ulin, calcium, and BH_4. BH_4 is a cofactor essential for the appropriate enzymatic activity of NOS. However, unusual situations (e.g., decreased levels of the substrate

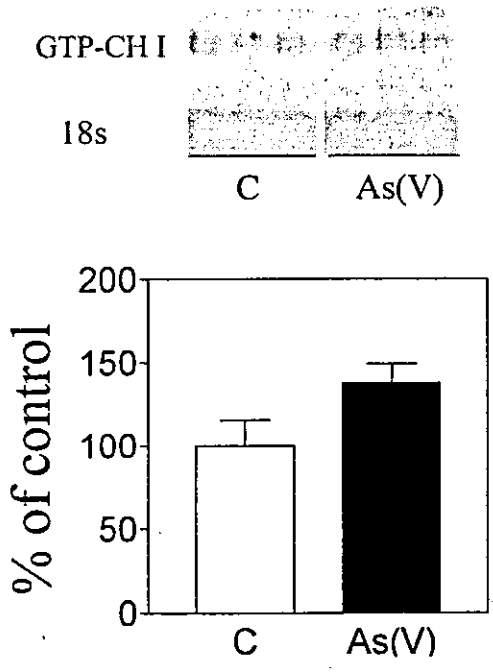

Fig. 6. Expression of GTP-CH I in cardiac tissue of rabbits. C = control; As(V) = arsenate. Northern blot analysis was performed using a GTP-CH I cDNA probe prepared according to the cDNA sequence of rat. Membranes were rehybridized with a probe for 18s ribosomal RNA (left). The mRNA levels were quantitated by radioanalytic scanning (right). Data represent mean ± SEM; $n = 3$ per group.

L-arginine or the cofactor BH_4), results in the uncoupling of NOS with subsequent enhanced production of reactive oxygen species (ROS) such as $O_2^{\bullet -}$ and H_2O_2, and diminished NO formation [24,27,56]. These observations led us to a hypothesis that prolonged exposure to inorganic arsenic may affect levels of BH_4 and possibly L-arginine, thereby reducing systemic NO production, as reflected in plasma metabolites, with a concomitant generation of ROS. Earlier work showed NO metabolites in serum were reduced in humans chronically exposed to high levels of As(V) [7]. The present results in rabbits show that the hepatic levels of BH_4 in animals exposed to As(V) were markedly reduced (~ 40%), whereas the levels of L-arginine, at least in cardiac tissue, were unaffected by As(V) exposure. Our data suggest that As(V) exposure may indeed cause an uncoupling of NOS by decreasing levels of cofactor, BH_4, but not through decreasing substrate, and that this uncoupling results in diminished NO production accompanied by enhanced production of ROS, as reflected by increased H_2O_2 in urine. Although additional work will be required, the present results indicate that disruption of NO production may be an indirect mechanism by which inorganic arsenic produces oxidative stress.

In the present research, we were unable to directly measure the level of BH_4 in vascular tissues, such as aortas or hearts, due to limited amounts of sample. But if uncoupling of NOS does, in fact, occur in endothelium during prolonged exposure of rabbits to arsenate, it was reasoned that use of an agent to increase intracellular calcium level in aortic rings of arsenate-exposed rabbits would bring about a significant vasoconstriction as this uncoupling reaction would produce $O_2^{\bullet -}$, which is known to act as an endothelium-derived contracting factor. Consistent with this notion, the calcium ionophore A23187 induced transient but significant contractions of the aortas of rabbits exposed to As(V), and not in controls, indicating that the aberrant vasoconstriction caused by prolonged As(V) exposure can occur through calcium. These results are consistent with the results of Wang et al. [57], who reported that calcium-mediated production of ROS play important role in arsenite-induced DNA adducts in mammalian cells. There are a variety of $O_2^{\bullet -}$-generating enzymes such as NAD(P)H oxidase, cyclooxygenase, lipoxygenase, and xanthine oxidase, as well as eNOS, all of which are functional in endothelial cells [58]. Barchowsky et al. [59] previously reported that low levels of arsenite cause increased reactive oxygen formation in vascular endothelial cells, and the overproduced reactive oxygen is likely to result from arsenite stimulation of NAD(P)H oxidase. However, NAD(P)H oxidase is not a calcium-dependent enzyme, suggesting that the enhanced calcium-mediated

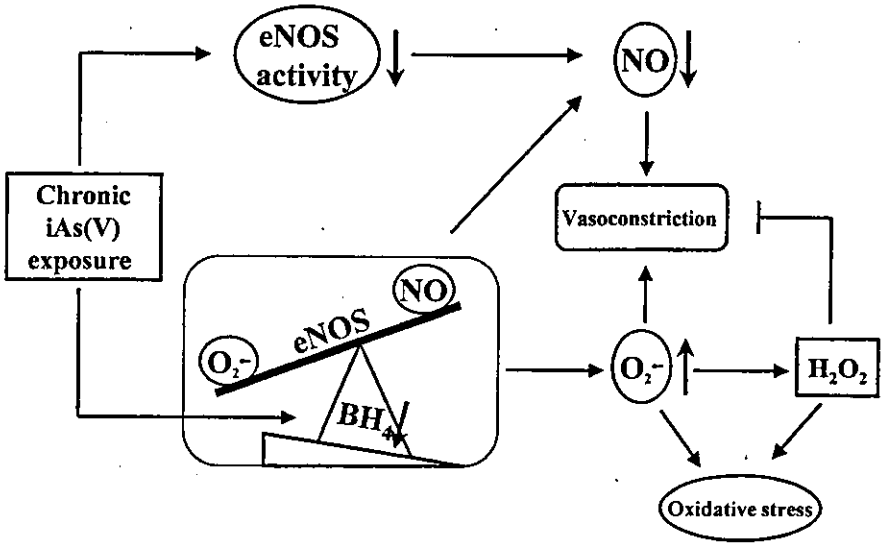

Fig. 7. A possible mechanism for the impairment of NO formation and induction of oxidative stress caused by chronic exposure to arsenate in drinking water.

aortic vasoconstriction occurs through disrupted NOS, but not NAD(P)H oxidase. Interestingly, the vasoconstriction of aortic rings induced through calcium release in As(V)-exposed rabbits was drastically attenuated by L-NAME, a specific inhibitor of NOS, and DPI, a general inhibitor of flavin enzymes including NOS, but not by cyclooxygenase or xanthine oxidase inhibitors, again suggesting the involvement of eNOS in the superoxide production. Taken together, these data suggest that an uncoupling of eNOS occurs from prolonged arsenic exposure, which promotes, at least in part, increased formation of $O_2^{\bullet-}$ by eNOS and $O_2^{\bullet-}$-induced vasoconstriction, as shown in Fig. 7. Therefore, both our cross-sectional human study in China [7,26] and the present experiments with rabbits suggest the possibility that As(V) uncouples NOS that may play an important role in the reduction of systemic NO production and increased oxidative stress. The hypersensitivity to vasoconstriction after As(V) exposure may also predispose to development of various vascular diseases.

Under physiological conditions, BH_4 is synthesized from GTP via a de novo pathway by three enzymes: GTP-CH I, 6-pyruvoyl-tetrahydropterin synthase, and sepiapterin reductase (SR) [60]. The committing step of the reaction is carried out by GTP-CH I. Alternatively, the synthesis of BH_4 can occur via a so-called salvage pathway with sepiapterin as a substrate, independent of GTP-CH I [60]. Enzymatic recycling of BH_4 is essential to ensure a continuous supply of BH_4. Two enzymes, pterin-4α-carbinolamine dehydratase (PCD) and dihydropteridine reductase, are involved in these processes [60]. In the current study, no significant change occurred in GTP-CH I gene expression in liver. Furthermore, As(V) exposure did not appear to affect PCD activity since no higher level of 7-biopterin, the co-product in BH_4 salvage, was detected in the urine of As(V)-exposed rabbits (data not shown). Thus, critical enzymes involved in the de novo production and salvage of BH_4 appear to be unaltered by prolonged As(V) exposure. Additional study will be required to define exactly how As(V) exposure reduces BH_4, but this appears to be a critical aspect to reduced NO production and increased ROS production.

ROS can decrease the bioavailability of NO, especially the radical $O_2^{\bullet-}$, which readily reacts with NO to form peroxynitrite ($ONOO^-$), a reactive and short-lived species that promotes oxidative molecular and tissue damage [61]. It has been reported that NO acts as a potent inhibitor of the lipid peroxidation chain reaction by scavenging propagatory lipid peroxyl radicals or various potential initiators of lipid peroxidation. On the other hand, $ONOO^-$ can initiate lipid peroxidation and oxidizing lipid soluble antioxidants [61,62]. In addition, both $O_2^{\bullet-}$ and H_2O_2 can be transformed into hydroxyl radicals ($^{\bullet}OH$), which can catalyze the production of vasoconstrictor prostanoids. These mediators act directly on vascular smooth muscle cells to induce contraction [63]. Therefore, other compounds derived from the excessive $O_2^{\bullet-}$ production seen in the present study after As(V) exposure, such as $ONOO^-$, also probably contributed to the transient constriction effects.

It has been well documented that $O_2^{\bullet-}$ can be transformed by SOD to H_2O_2, which causes vascular relaxation by activation of soluble guanylate cyclase

and increases in the level of cGMP in smooth muscle cells [64] and endothelium-derived hyperpolarizing factor (EDHF) activity [65]. In the present research, As(V) exposure had no significant effects on the aorta relaxation in response to ACh or A23187, though a significant decrease of systemic NO production was observed. This may be associated with increased level of H_2O_2 in vessels accompanied with $NO/O_2^{\bullet -}$ balance shift. NOS-catalyzed production of H_2O_2 may initially serve as a compensatory mechanism in conditions associated with low concentrations of BH_4. However, H_2O_2 is also a powerful, although relatively slow, oxidant in its reactivity toward biological compounds [66]. In this regard, H_2O_2-derived $^{\bullet}OH$ is often toxic through the direct peroxidation of either lipids or proteins [67]. Thus, a prolonged increase in intracellular production of H_2O_2 may lead to oxidative vascular injury. Indeed, we recently have provided evidence that chronic exposure of humans to arsenic in drinking water resulted in induction of oxidative stress, as indicated by the enhancement of lipid peroxides [26]. The disrupted NO metabolism observed in human [7] and rabbits (present study) could lead to vascular injury and, eventually, overt diseases.

In conclusion, our current findings suggest that prolonged As(V) exposure impaired endothelial function through decreased NO bioavailability due to either reduced production, or inactivation by elevated $O_2^{\bullet -}$ and its derived oxidants. The disruption of NO production may increase oxidative stress, which could play a fundamental role in the pathogenesis of chronic arsenic poisoning, including vascular diseases and possibly cancer. In particular, impaired bioavailability of BH_4 may be associated with As(V)-induced endothelium dysfunction. Considering the controlling role of BH_4 in eNOS-catalyzed NO and/or $O_2^{\bullet -}$ generation, BH_4 levels in vivo may provide an important biomarker of chronic arsenic poisoning, and enhancing these levels may provide a basis for therapeutic intervention.

Acknowledgements — This work was supported in part by funding from Japan-China Medical Association and China Nature Science Foundation (#30000142 to J.B.P.) and by Grants-in-Aids (#13576029 to Y.K., #13680620 and #13575036 to N.S., #13576018 to H.Y.) for scientific research from the Ministry of Education, Science and Culture of Japan. We wish to thank Dr. A. K. Suzuki, Research Team for Health Effects of Air Pollutants, National Institute for Environmental Studies, Japan; Dr. T. Yoshida, Department of Hygiene, Asahikawa Medical University, Japan; Dr. S. Li, National Institute for Environmental Studies, Japan; Ms. Y. Nakai, Analytical Instruments Division, JEOL Ltd., Japan; Dr. Y. Ishii, Department of Environmental Medicine, Institute of Community Medicine, University of Tsukuba, Japan for their excellent contribution to this work. We also thank Drs. Jie Liu and William Achanzar for their critical comments and assistance during the preparation of this manuscript.

REFERENCES

[1] Cullen, W. R.; Reimer, K. J. Arsenic speciation in the environment. *Chem. Rev.* **89**:713–774; 1989.
[2] IARC. International agency for research on cancer monographs on the evaluation of carcinogenic risks to humans: supplement 7. Overall evaluations of carcinogenicity: an updating of *IARC Monographs* volumes 1–42, p. 100–106. Lyon, France: IARC Scientific Publications; 1987.
[3] Aposhian, H. V. Biochemical toxicology of arsenic. *Rev. Biochem. Toxicol.* **10**:265–299; 1989.
[4] Hopenhayn-Rich, C.; Browning, S. R.; Hertz-Picciotto, I.; Ferreccio, C.; Peralta, C.; Gibb, H. Chronic arsenic exposure and risk of infant mortality in two areas of Chile. *Environ. Health Perspect.* **19**:103–105; 1983.
[5] Hernández-Zavala, A.; Razo, L. M. D.; García-Vargas, G. G.; Aguilar, C.; Borja, V. H.; Albores, A.; Cebrián, M. E. Altered activity of heme biosynthesis pathway enzymes in individuals chronically exposed to arsenic in Mexico. *Arch. Toxicol.* **73**:90–95; 1999.
[6] Tseng, W. P.; Chu, H. M.; How, S. W.; Fong, J. M.; Lin, C. S.; Yeh, S. Prevalence of skin cancer in an endemic area of chronic arsenicism in Taiwan. *J. Natl. Cancer Inst.* **40**:453–463; 1968.
[7] Pi, J. B.; Kumagai, Y.; Sun, G. F.; Yamauchi, H.; Yoshida, T.; Iso, H.; Endo, A.; Yu, L.; Yuki, K.; Miyauchi, T.; Shimojo, N. Decreased serum concentrations of nitric oxide metabolites among Chinese in an endemic area of chronic arsenic poisoning in Inner Mongolia. *Free. Radic. Biol. Med.* **28**:1137–1142; 2000.
[8] Gebel, T. W. Arsenic and drinking water contamination. *Science* **283**:1458–1459; 1999.
[9] Tondel, M.; Rahman, M.; Magnuson, A.; Chowdhury, I. A.; Faruquee, M. H.; Ahmad, S. A. The relationship of arsenic levels in drinking water and the prevalence rate of skin lesions in Bangladesh. *Environ. Health Perspect.* **107**:727–729; 1999.
[10] Kurttio, P.; Pukkala, E.; Kahelin, H.; Auvinen, A.; Pekkanen, J. Arsenic concentrations in well water and risk of bladder and kidney cancer in Finland. *Environ. Health Perspect.* **107**:705–710; 1999.
[11] Borzsonyi, M.; Bereczky, A.; Rudnai, P.; Csanady, M.; Horvath, A. Epidemiological studies on human subjects exposed to arsenic in drinking water in Southwest Hungary. *Arch. Toxicol.* **66**:77–78; 1992.
[12] World Health Organization. Environmental health criteria, vol. 18: Arsenic. Geneva, Switzerland: World Health Organization; 1981:43–102.
[13] Sun, G. F.; Pi, J. B.; Li, B.; Guo, X.; Yamauchi, H.; Yoshida, T. Introduction of present arsenic research in China. The Fourth International Conference on Arsenic Exposure and Health Effects. June 2000. San Diego, CA, USA.
[14] Breslin, K. Arsenic in Asia. *Environ. Health Perspect.* **108**:224; 2000.
[15] Chen, C. J.; Hsueh, Y. M.; Lai, M. S.; Shyu, M. P.; Chen, S. Y.; Wu, M. M.; Kuo, T. K.; Tai, T. Y. Increased prevalence of hypertension and long-term arsenic exposure. *Hypertension* **25**: 53–60; 1995.
[16] Lagerkvist, B. E. A.; Linderholm, H.; Nordberg, G. F. Arsenic and Raynaud's phenomenon: vasospastic tendency and excretion of arsenic in smelter workers before and after the summer vacation. *Int. Arch. Occup. Environ. Health* **60**:361–364; 1988.
[17] Engel, R. R.; Hopenhayn-Rich, C.; Receveur, O.; Smith, A. H. Vascular effects of chronic arsenic exposure: a review. *Epidemiol. Rev.* **16**:184–209; 1994.
[18] Chen, C. J. Blackfoot disease. *Lancet* **336**:442; 1990.
[19] Tseng, C. H.; Chong, C. K.; Chen, C. J.; Tai, T. Y. Lipid profile and peripheral vascular disease in arseniasis-hyperendemic villages in Taiwan. *Angiology* **48**:321–335; 1997.
[20] Wu, M. M.; Kuo, T. L.; Hwang, Y. H.; Chen, C. J. Dose-response relation between arsenic concentration in well water and mortality from cancers and vascular diseases. *Am. J. Epidemiol.* **130**:1123–1132; 1989.

[21] Chen, C. J.; Kuo, T. L.; Wu, M. M. Arsenic and cancers. *Lancet* 1:414–415; 1988.
[22] Rees, D. D.; Palmer, R. M. J.; Moncada, S. Role of endothelium-derived nitric oxide in the regulation of blood pressure. *Proc. Natl. Acad. Sci. USA* 86:3375–3378; 1989.
[23] Moncada, S.; Higgs, A. The L-arginine-nitric oxide pathway. *N. Engl. J. Med.* 329:2002–2012; 1993.
[24] Böger, R. H.; Bode-Böger, S. M.; Mügge, A.; Kienke, S.; Brandes, R.; Dwenger, A.; Frölich, J. C. Supplementation of hypercholesterolemic rabbits with L-arginine reduces the vascular disease of superoxide anions and restores NO production. *Atherosclerosis* 117:273–284; 1995.
[25] Böger, R. H.; Bode-Böger, S. M.; Thiele, W.; Junker, W.; Alexander, K.; Frölich, J. C. Biochemical evidence for impaired nitric oxide synthesis in patients with peripheral arterial occlusive disease. *Circulation* 95:2068–2074; 1997.
[26] Pi, J. B.; Yamauchi, H.; Kumagai, Y.; Sun, G. F.; Yoshida, T.; Aikawa, H.; Hopenhayn-Rich, C.; Shimojo, N. Evidence for induction of oxidative stress caused by chronic exposure of Chinese residents to arsenic contained in drinking water. *Environ. Health Perspect.* 110:331–336; 2002.
[27] Werner, E. R.; Werner-Felmayer, G.; Wachter, H.; Mayer, B. Biosynthesis of nitric oxide: dependence on pteridine metabolism. *Rev. Physiol. Biochem. Pharmacol.* 127:97–135; 1995.
[28] Heinzel, B.; John, M.; Klatt, P.; Böhme, E.; Mayer, B. Ca2+/calmodulin-dependent formation of hydrogen peroxide by brain nitric oxide synthase. *Biochem. J.* 281:627–630; 1992.
[29] Harrison, D. G. Cellular and molecular mechanisms of endothelial cell dysfunction. *J. Clin. Invest.* 100:2153–2157; 1997.
[30] Kwon, N. S.; Nathan, C. F.; Stuehr, D. J. Reduced biopterin as cofactor in the generation of nitrogen oxides by murine macrophages. *J. Biol. Chem.* 264:20446–20501; 1989.
[31] Reif, A.; Fröhlich, L. G.; Kotsonis, P.; Frey, A.; Bömmel, H. M.; Wink, D. A.; Pfleiderer, W.; Schmidt, H. H. Tetrahydrobiopterin inhibits monomerization and is consumed during catalysis in neuronal NO synthase. *J. Biol. Chem.* 274:24921–24929; 1999.
[32] Vallance, P.; Leone, A.; Calver, A.; Collier, J.; Moncada, S. Endogenous dimethylarginine as an inhibitor of nitric oxide synthesis. *J. Cardiovasc. Pharmacol.* 20:S60–S62; 1992.
[33] Aisaka, K.; Gross, S. S.; Griffith, O. W.; Levi, R. N^G-methylarginine, an inhibitor of endothelium-derived nitric oxide synthesis, is a potent pressor agent in the guinea pig: does nitric oxide regulate blood pressure in vivo? *Biochem. Biophys. Res. Commun.* 160: 881–886; 1989.
[34] Bode-Böger, S. M.; Böger, R. H.; Kienke, S.; Junker, W.; Frölich, J. C. Elevated L-arginine/dimethylarginine ratio contributes to enhanced systemic NO production by dietary L-arginine in hypercholesterolemic rabbits. *Biochem. Biophys. Res. Commun.* 219:598–603; 1996.
[35] Usui, M.; Matsuoka, H.; Miyazaki, H.; Ueda, S.; Okuda, S.; Imaizumi, T. Increased endogenous nitric oxide synthase inhibitor in patients with congestive heart failure. *Life Sci.* 62:2425–2430; 1998.
[36] Schallreuter, K. U.; Wood, J. M.; Pittelkow, M. R.; Gütlich, M.; Lemke, K. R.; Rödl, W.; Swanson, N. N.; Hitzemann, K.; Ziegler, I. Regulation of melanin biosynthesis in the human epidermis by tetrahydrobiopterin. *Science* 263:1444–1446; 1994.
[37] Delgado, J. M.; Dufour, L.; Grimaldo, J. I.; Carrizales, L.; Rodríguez, V. M.; Jiménez-Capdeville, M. E. Effects of arsenite on central monoamines and plasmatic levels of adrenocorticotropic hormone (ACTH) in mice. *Toxicol. Lett.* 117:61–67; 2000.
[38] Rodríguez, V. M.; Dufour, L.; Carrizales, L.; Díaz-Barriga, F.; Jiménez-Capdeville, M. E. Effects of oral exposure to mining waste on in vivo dopamine release from rat striatum. *Environ. Health Perspect.* 106:487–491; 1998.
[39] Nagaraja, T. N.; Desiraju, T. Regional alterations in the levels of brain biogenic amines, glutamate, GABA, and GAD activity due to chronic consumption of inorganic arsenic in developing and adult rats. *Bull. Environ. Contam. Toxicol.* 50:100–107; 1993.
[40] McDorman, E. W.; Collins, B. W.; Allen, J. W. Dietary folate deficiency enhances induction of micronuclei by arsenic in mice. *Environ. Mol. Mutagen.* 40:71–77; 2002.
[41] Kaufman, S. Some metabolic relationships between biopterin and folate: implication for the "methyl trap hypothesis". *Neurochem. Res.* 16:1031–1036; 1991.
[42] Maiorino, R. M.; Aposhian, H. V. Dimercaptan metal-binding agents influence the biotransformation of arsenite in the rabbit. *Toxicol. Appl. Pharmacol.* 77:240–250; 1985.
[43] Cosentino, F.; Sill, J. C.; Katusic, Z. S. Role of superoxide anions in the mediation of endothelium-dependent contractions. *Hypertension* 23:229–235; 1993.
[44] Green, L. C.; Wagner, D. A.; Glogowski, J.; Skipper, P. L.; Wishnok, J. S.; Tannenbaum, S. R. Analysis of nitrite, and [^{15}N]nitrate in biological fluids. *Anal. Biochem.* 26:131–138; 1982.
[45] Long, L. H.; Evans, P. J.; Halliwell, B. Hydrogen peroxide in human urine: implications for antioxidant defense and redox regulation. *Biochem. Biophys. Res. Commun.* 262:605–609; 1999.
[46] Furchgott, R. F.; Zawadzki, J. The obligatory role of endothelial cells in the relaxation of arterial smooth muscle by acetylcholine. *Nature* 288:373–376; 1980.
[47] Fukushima, T.; Nixon, J. C. Analysis of reduced forms of biopterin in biological tissues and fluids. *Anal. Biochem.* 102:176–188; 1980.
[48] Stea, B.; Halpern, R. M.; Halpern, B. C.; Smith, R. A. Quantitative determination of pterins in biological fluids by high-performance liquid chromatography. *J. Chromatogr.* 188:363–375; 1980.
[49] Gütlich, M.; Schott, K.; Werner, T.; Bacher, A.; Ziegler, I. Species and tissue specificity of mammalian GTP cyclohydrolase I messenger RNA. *Biochim. Biophys. Acta* 1171:133–140; 1992.
[50] Pi, J. B.; Kumagai, Y.; Sun, G. F.; Shimojo, N. Improved method for simultaneous determination of L-arginine and its mono- and dimethylated metabolites in biological samples by high-performance liquid chromatography. *J. Chromatgr. B Biomed. Sci. Appl.* 742:199–203; 2000.
[51] Bradford, M. M. A rapid and sensitive method for the quantitation of microgram quantities of protein utilizing the principle of protein-dye binding. *Anal. Biochem.* 72:248–254; 1997.
[52] Yamauchi, H.; Yamamura, Y. Metabolism and excretion of orally administered dimethylarsinic acid in the hamster. *Toxicol. Appl. Pharmacol.* 74:134–140; 1984.
[53] de Zwart, L. L.; Meerman, J. H.; Commandeur, J. N.; Vermeulen, N. P. Biomarkers of free radical damage applications in experimental animals and in humans. *Free Radic. Biol. Med.* 26:202–226; 1999.
[54] Halliwell, B.; Clement, M. V.; Long, L. H. Hydrogen peroxide in the human body. *FEBS Lett.* 486:10–13; 2000.
[55] Denninger, J. W.; Marletta, M. A. Guanylate cyclase and the NO/cGMP signaling pathway. *Biochim. Biophys. Acta* 1411:334–350; 1999.
[56] Xia, Y.; Tsai, A. L.; Berka, V.; Zweier, J. L. Superoxide generation by endothelial nitric oxide synthase: the influence of cofactors. *Proc. Natl. Acad. Sci. USA* 95:9220–9225; 1998.
[57] Wang, T. S.; Hsu, T. Y.; Chung, C. H.; Wang, A. S. S.; Bau, D. T.; Jan, K. Y. Arsenite induces oxidative DNA adducts and DNA-protein cross-links in mammalian cells. *Free Radic. Biol. Med.* 31:321–330; 2001.
[58] Wolin, M. S. Interactions of oxidants with vascular signaling systems. *Arterioscler. Thromb. Vasc. Biol.* 20:1430–1442; 2000.
[59] Barchowsky, A.; Klei, L. R.; Dudek, E. J.; Swartz, H. M.; James, P. E. Stimulation of reactive oxygen, but not reactive nitrogen species, in vascular endothelial cells exposed to low levels of arsenite. *Free Radic. Biol. Med.* 27:1405–1412; 1999.
[60] Thöny, B.; Auerbach, G.; Blau, N. Tetrahydrobiopterin biosyn-

thesis, regeneration and functions. *Biochem. J.* **347**:1–16; 2000.
[61] Radi, P.; Peluffo, G.; Alvarez, M. N.; Naviliat, M.; Cayota, A. Unraveling peroxynitrite formation in biological system. *Free Radic. Biol. Med.* **30**:463–488; 2001.
[62] Hogg, N.; Kalyanaraman, B. Nitric oxide and lipid peroxidation. *Biochim. Biophys. Acta* **1411**:378–384; 1999.
[63] Auch-Schwelk, W.; Katusic, Z. S.; Vanhoutte, P. M. Contractions to oxygen-derived free radicals are augmented in aorta of the spontaneously hypertensive rat. *Hypertension* **13**:859–864; 1989.
[64] Matoba, T.; Shimokawa, H.; Nakashima, M.; Hirakawa, Y.; Mukai, Y.; Hirano, K.; Kanaide, H.; Takeshita, A. Hydrogen peroxide is an endothelium-derived hyperpolarizing factor in mice. *J. Clin. Invest.* **106**:1521–1530; 2000.
[65] Marshall, J. J.; Kontos, H. A. Endothelium-derived relaxing factors: a perspective from in vivo data. *Hypertension* **16**:371–386; 1990.
[66] Freeman, B. A.; Crapo, J. D. Biology of disease: free radicals and tissue injury. *Lab. Invest.* **47**:412–425; 1982.
[67] Vanhoutte, P. M. Endothelium-derived free radicals: for worse and for better. *J. Clin. Invest.* **107**:23–25; 2001.

ABBREVIATIONS

A23187—calcium ionophore A23187
ACh—acetylcholine
BH_4-(6*R*)-5,6,7,8-tetrahydro-L-biopterin
cNOS—constitutive nitric oxide synthase
DPI—diphenyleneiodonium
eNOS—endothelial nitric oxide synthase
H_2O_2—hydrogen peroxide
iAs(V)—inorganic pentavalent arsenate
iAs-inorganic arsenic
L-NAME—N^Gnitro-L-arginine methyl este
NO—nitric oxide
NOS—nitric oxide synthase
$O_2^{\bullet -}$—superoxide
PE—phenylephrine
SOD-Cu,Zn—Superoxide dismutase

Oncogene (2003) 22, 9275–9281

www.nature.com/onc

SHORT REPORTS

Nrf2 regulates the sensitivity of death receptor signals by affecting intracellular glutathione levels

Naoki Morito[1], Keigyou Yoh[2], Ken Itoh[1,3], Aki Hirayama[2], Akio Koyama[2], Masayuki Yamamoto[1,3] and Satoru Takahashi*[,1,4]

[1]*Institute of Basic Medical Sciences, University of Tsukuba, 1-1-1 Tennodai, Tsukuba, Ibaraki 305-8575, Japan;* [2]*Institute of Clinical Medicine, University of Tsukuba, 1-1-1 Tennodai, Tsukuba, Ibaraki 305-8575, Japan;* [3]*Center for Tsukuba Advanced Research Alliance, University of Tsukuba, 1-1-1 Tennodai, Tsukuba, Ibaraki 305-8575, Japan and* [4]*Laboratory Animal Resource Center, University of Tsukuba, 1-1-1 Tennodai, Tsukuba, Ibaraki 305-8575, Japan*

Nrf2 is a basic leucine zipper transcriptional activator that is essential for the coordinate transcriptional induction of various antioxidant drug-metabolizing enzymes. Numerous studies have firmly established Nrf2's importance in protection from oxidative stress and certain chemical insults. Given the protective function of Nrf2, surprisingly few studies have focused on the relationship between Nrf2 and apoptosis. Therefore, we analysed how Nrf2 influences Fas signaling using Nrf2-deficient T cells. At a concentration of 1 μg/ml, the anti-Fas antibody induced 60% of cell death in Nrf2-deficient cultured thymocytes while, using the same treatment, only 40% of Nrf2 wild-type thymocytes died ($P<0.05$). Nrf2 deficiency enhances the sensitivity of Fas-mediated apoptosis in T cells. Next we examined the effect of Nrf2 deficiency during hepatocellular apoptosis *in vivo*. In comparison to wild-type mice, Nrf2-deficient mice displayed more severe hepatitis after induction with the anti-Fas antibody or tumor necrosis factor (TNF)-α. The enhanced sensitivity to anti-Fas or TNF-α stimulation was restored by preadministration of glutathione ethyl monoester, a compound capable of passing the cell membrane and upregulating the intracellular levels of glutathione. The results indicated that Nrf2 activity regulates the sensitivity of death signals by means of intracellular glutathione levels.

Oncogene (2003) **22,** 9275–9281. doi:10.1038/sj.onc.1207024

Keywords: Nrf2; oxidative stress; apoptosis; Fas; TNF-receptor I

NF-E2 related factor 2 (Nrf2) was originally defined as a basic leucine zipper (b-Zip) transcriptional activator that recognizes the nuclear factor erythroid 2 (NF-E2)-binding site (Moi *et al.*, 1994; Itoh *et al.*, 1995). Nrf2 is essential for the coordinate transcriptional induction of various antioxidant and phase II drug-metabolizing enzymes through the antioxidant response element/electrophile response element (ARE/EpRE) (Itoh *et al.*, 1997, 1999). ARE/EpRE sequences have been characterized within the proximal regulatory sequences of genes encoding the antioxidant enzymes glutathione *S*-transferase (GST) (Rushmore *et al.*, 1990), NAD(P)H quinone oxidoreductase (NQO1) (Favreau and Pickett, 1991), heme oxygenase-1 (HO-1) (Prestera *et al.*, 1995), γ-glutamylcysteine synthetase (Chan and Kwong, 2000), and cystine membrane transporter (system X_c^-) (Ishii *et al.*, 2000). The ARE also regulates a wide range of metabolic responses to oxidative stress caused by reactive oxygen species (ROS) or electrophiles (Ishii *et al.*, 2000). As a consequence of inadequate induction of these molecules, Nrf2-deficient mice are sensitive to high oxidative stress and drug-induced stress (Ishii *et al.*, 2000; Enomoto *et al.*, 2001; Cho *et al.*, 2002).

Glutathione (L-γ-glutamyl-cysteinyl-glycine, GSH) is a tripeptide, intracellular, nonprotein thiol that has a central role in sulfhydryl homeostasis. GSH serves as the major cytosolic antioxidant and defends against xenobiotics by acting as a substrate during phase II conjugation reactions (Jones *et al.*, 1986; Meister, 1992). Numerous cellular functions are modulated by the glutathione disulfide system, including regulation of enzymes vital to metabolism, cell growth, gene transcription, and apoptosis (Uhlig and Wendel, 1992; Droge *et al.*, 1994; Hall, 1999). Therefore, cells tightly regulate the synthesis, utilization, and export of GSH. The intracellular concentration of GSH is maintained within the millimolar range under normal conditions (Anderson, 1997). The synthesis of GSH is achieved by the consecutive action of the ATP-dependent enzymes, γ-glutamylcysteine synthetase and glutathione synthetase. It was reported that levels of both these key enzymes are affected by the activity of Nrf2 (Chan and Kwong, 2000). In addition, the expression of system X_c^- is controlled by Nrf2 (Ishii *et al.*, 2000). System X_c^- regulates the concentration of intracellular cystine, a component substrate for GSH synthesis. Based upon these findings, Nrf2 is thought to be one of the main regulators of intracellular GSH levels.

The cytokine receptor Fas (APO-1/CD95) belongs to the tumor necrosis factor (TNF)/nerve growth factor

*Correspondence: S Takahashi, Institute of Basic Medical Sciences, University of Tsukuba, 1-1-1 Tennodai, Tsukuba, Ibaraki 305-8575, Japan; E-mail: satoruta@md.tsukuba.ac.jp
Received 1 March 2003; revised 19 July 2003; accepted 21 July 2003

receptor superfamily. Certain members of this family, including Fas, are referred to as death receptors since they share a cytoplasmic death domain involved in apoptotic signaling (Schulze-Osthoff *et al.*, 1998). Fas is expressed by lymphoid and nonlymphoid cells and is regarded as a principal trigger for apoptotic cell death of lymphoid cells and hepatocytes (Galle *et al.*, 1995; Nagata, 1997). In both human and murine liver, Fas and TNF-receptor I (TNF-RI) can independently trigger apoptosis. Indeed, the administration of an activating anti-Fas antibody to mice leads to lethal liver destruction within hours due to extensive apoptosis of hepatocytes (Ogasawara *et al.*, 1993; Leist *et al.*, 1996). Upon ligand binding and trimerization of Fas, the intracellular death domain of the receptor associates with several proteins forming a death-inducing signaling complex (DISC) through which the recruitment and activation of caspase-8 is initiated (Medema *et al.*, 1997; Schulze-Osthoff *et al.*, 1998). This event, in turn, triggers a cascade of proteolytic interconversions of procaspases, including downstream caspases such as caspase-3 and -7, which finally execute the proteolytic cleavage of various structural and signal proteins (Zhivotovsky *et al.*, 1997; Hirata *et al.*, 1998; Thronberry and Lazebnik, 1998; Widmann *et al.*, 1998). The ultimate outcome of this cascade is apoptosis. TNF-α also plays an integral role in the injury and cell death that occurs in hepatocytes following toxin-induced liver damage. TNF-α-induced cell death is mainly transduced through TNF-RI and the signaling pathway is similar to Fas-induced apoptosis (Schulze-Osthoff *et al.*, 1998).

There have been several reports describing the modulation of Fas- or TNF-RI-mediated apoptosis by GSH. According to these reports, acute GSH depletion induced insensitivity to death receptor stimulation (Hentze *et al.*, 1999, 2000), while during prolonged GSH depletion increased death receptor-mediated apoptosis was observed (Chiba *et al.*, 1996; Colell *et al.*, 1998; Xu *et al.*, 1998). The reports strongly indicated that Nrf2 activity may influence the sensitivity of death signaling, but the relationship between Nrf2 and apoptotic signaling was not clearly characterized. Recently, Kotlo *et al.* (2003) demonstrated that inactivation of Nrf2 by antisense or by using a membrane-permeable dominant-negative polypeptide sensitized cells while, conversely, overexpression of Nrf2 protected cells from Fas-induced apoptosis. In addition, they demonstrated that *N*-acetyl-L-cysteine (NAC), a precursor to GSH, protected cells from Fas-mediated killing in HeLa cells.

In this report, we have analysed the sensitivity of death signaling (Fas- and TNF-α-mediated apoptosis) in Nrf2-deficient mice and demonstrated a high susceptibility to death signals *in vivo*. Preadministration of glutathione ethyl monoester (GSH-OEt), which upregulates GSH, canceled the observed enhanced sensitivity. This indicates that the low intracellular GSH levels that resulted from Nrf2 deficiency are a primary cause for the susceptibility.

To investigate the role of Nrf2 in Fas-mediated apoptosis, cultured Nrf2-deficient thymocytes were examined in the presence of an agonistic anti-Fas antibody. Our results showed that a deficiency in Nrf2 increased the percentage of apoptotic thymocytes following Fas stimulation (Figure 1a). The anti-Fas antibody, at a concentration of 1 μg/ml, induced 60% of cell death in thymocytes from Nrf2-deficient mice while, using the same treatment, 40% of cells from wild-type mice died ($P<0.05$). Recently, it has been found that prolonged GSH depletion enhances Fas-mediated apoptosis (Haouzi *et al.*, 2001). We and others reported that intracellular GSH levels were reduced in Nrf2-deficient cells (Chan and Kwong, 2000; Ishii *et al.*, 2000). Therefore, we suspected that the observed sensitivity of cultured thymocytes to Fas-mediated apoptosis could be due to a depletion of cellular GSH levels resulting from a deficiency in Nrf2. The administration of GSH-OEt can increase the intracellular GSH concentration *in vitro* and *in vivo* (Chen *et al.*, 2001; Rahman *et al.*, 2001). Therefore, we

Figure 1 Effects of Nrf2 deficiency on cultured thymocytes treated with an agonistic anti-Fas antibody. The generation of Nrf2-deficient mice has been previously described (Itoh *et al.*, 1997). The present study utilized 12-week-old mice from the same litters with an ICR background. Freshly isolated thymocytes from Nrf2-deficient, chronically treated with BSO (6 weeks) and untreated wild-type mice were incubated overnight with the indicated concentrations of the anti-Fas antibody. The cells were washed with DMEM supplemented with 10% heat-inactivated fetal bovine serum, 0.5 mM 2-mercaptoethanol, 2 mM glutamine, 1 mM HEPES (pH 7.4), and antibiotics (all from Invitrogen). The cells were again washed in medium before use in subsequent tissue culture experiments. The cells (1×10^6/ml) were incubated with various concentrations of the anti-Fas antibody (Jo-2, BD Bioscience) for 12 h. Cell viability was determined by trypan blue exclusion. The cells were preincubated with GSH-OEt (obtained from WAKO) (2 mM for 15–20 min) to increase the intracellular pool of GSH. Each Bar represents the mean $\pm$ s.d. (a) Survival rate of Nrf2-deficient thymocytes after Fas stimulation was significantly decreased ($P<0.05$) compared with wild-type thymocytes. Nrf2 deficiency increased the percentage of apoptotic thymocytes after Fas stimulation. *Significant difference from wild-type thymocytes ($P<0.05$). (b) GSH-OEt protected Nrf2-deficient thymocytes against Fas-mediated apoptosis. Thymocytes were preincubated with 2 mM GSH-OEt. There was no significant difference in the survival rate between Nrf2-deficient and wild-type thymocytes with 2 mM GSH-OEt. (c) The survival of wild-type thymocytes chronically treated with BSO was significantly decreased after Fas stimulation ($P<0.05$) compared with untreated wild-type thymocytes. BSO, a specific GSH synthesis inhibitory agent, increased the percentage of apoptotic thymocytes after Fas stimulation, similar to Nrf2 deficiency. **Significant difference from BSO-untreated wild-type thymocytes ($P<0.05$). (d) GSH-OEt protected thymocytes that were chronically treated with BSO against Fas-mediated apoptosis. There was no significant difference in the survival rate between BSO-treated and untreated wild-type thymocytes with 2 mM GSH-OEt. (e) GSH levels of thymocytes were examined pre- and post-anti-Fas antibody administration. GSH levels were measured using a Total Glutathione Quantification Kit (DOJINDO). The GSH levels of Nrf2-deficient thymocytes were significantly reduced compared to wild-type thymocytes, being decreased to almost the same level as that of BSO-treated thymocytes. GSH-OEt addition increased the GSH levels of Nrf2-deficient and BSO-treated thymocytes to almost the same level as that of Nrf2 wild-type thymocytes. #Significant difference from untreated wild-type thymocytes ($P<0.05$)

examined the effect of GSH-OEt treatment on Fas-mediated apoptosis in Nrf2-deficient thymocytes. The addition of GSH-OEt to Nrf2-deficient thymocytes re-established the sensitivity of Fas-mediated apoptosis to the level of wild-type mice thymocytes (Figure 1b). These results suggest that the enhanced sensitivity of the Fas signal in Nrf2-deficient thymocytes was due to a decrease in the intracellular GSH levels. However, due to the complicated nature of the GSH system, it is not possible to exclude the possibility that the administered GSH affected the adequate induction of some alternative adaptor molecule(s), whose function could be to prevent Fas-mediated apoptosis. To confirm the hypothesis that the enhanced sensitivity of the Fas signal was due to a decrease in the intracellular GSH levels, we analysed mice chronically treated

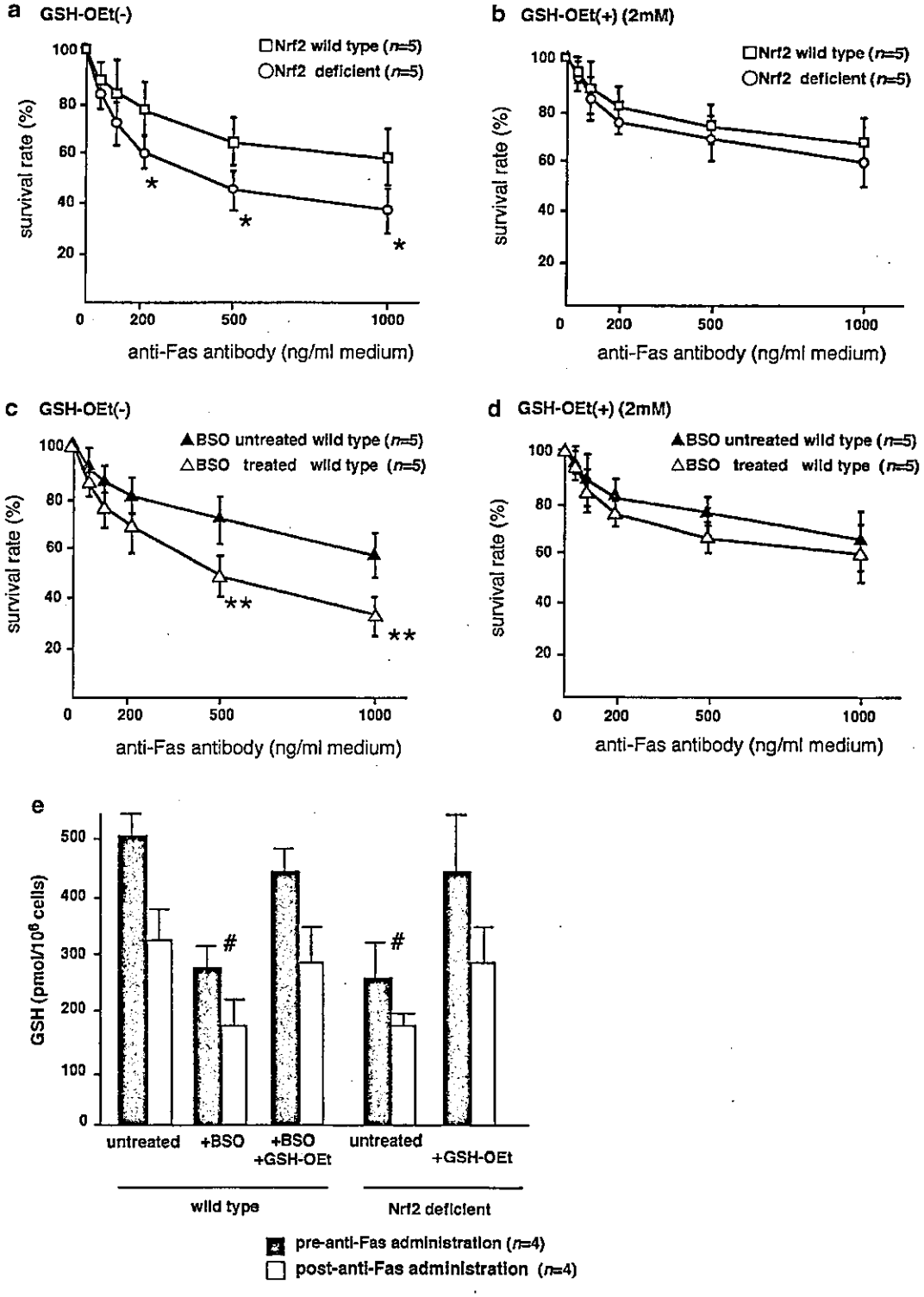

with buthionine sulfoximine (BSO). BSO is a specific GSH synthesis inhibitor that when administered to mice serves as a model of chronic GSH depletion (Srivastava *et al.*, 2000). Wild-type mice were given water supplemented with BSO (400 mg/kg/day) for 6 weeks. After 6 weeks, thymocytes were isolated from BSO-treated and control (untreated) wild-type mice. Analyses showed that Fas stimulation resulted in a larger percentage of apoptotic cells among BSO-treated thymocytes compared to wild-type controls (Figure 1c). Furthermore, the addition of GSH-OEt to BSO-treated thymocytes re-established the sensitivity of Fas-mediated apoptosis to the level of BSO-untreated mice thymocytes (Figure 1d). These results support the hypothesis that chronic GSH depletion enhances Fas-mediated apoptosis *in vitro*.

In the same experiment, we also determined the intracellular levels of GSH of thymocytes (Figure 1e). The GSH level of Nrf2-deficient thymocytes was decreased to almost the same level as that of BSO-treated wild-type thymocytes. GSH-OEt addition increased the GSH levels of Nrf2-deficient and BSO-treated thymocytes to the same level as that of Nrf2 wild-type thymocytes. These results also support the hypothesis that chronic GSH depletion enhanced Fas-mediated apoptosis *in vitro*.

It is well known that the administration of anti-Fas antibody to mice can induce fulminant hepatitis as a result of Fas-mediated apoptosis (Ogasawara *et al.*, 1993). The effect of hepatocellular apoptosis *in vivo* triggered by the anti-Fas antibody in Nrf2-deficient mice was examined. The anti-Fas antibody (Jo-2, 2 μg/mouse) was administered intraperitoneally to Nrf2-deficient and wild-type mice. Serum alanine aminotransferase (ALT) activities were determined as indices of hepatotoxicity. Serum ALT activity after Fas stimulation was significantly increased in Nrf2-deficient mice compared to Nrf2 wild-type mice ($P<0.05$) (Table 1). At 12 h after anti-Fas antibody administration, ALT activity in sera from Nrf2-deficient mice had increased to over 10 000 IU/l, while that of wild-type mice was around 5000 IU/l. Three out of five Nrf2-deficient mice were already dead at 8 h after injection. To prove that the enhancement of hepatitis in Nrf2-deficient mice was also due to a decrease in intracellular GSH levels, GSH-OEt was administered before anti-Fas antibody injection. The addition of GSH-OEt blocked the enhancement of Fas-induced fulminant hepatitis, suggesting that a

Table 1 Hepatotoxicity and lethality in Nrf2-deficient mice induced by the anti-Fas antibody

		ALT (IU/l)			*Survival rate (survived/all)*		
Treatment	*Time (h)*	*Nrf2 deficient*	*Wild type*	*BSO-treated wild type*	*Nrf2 deficient*	*Wild type*	*BSO-treated wild type*
GSH-OEt(−) anti-Fas	0	42±9	35±8	37±4	5/5	5/5	5/5
GSH-OEt(−) anti-Fas	4	1301±329*	626±100	1273±240*	5/5	5/5	5/5
GSH-OEt(−) anti-Fas	8	8110±2101*	3560±1175	8642±2346*	3/5	5/5	5/5
GSH-OEt(−) anti-Fas	12	12566±4848*	4582±835	9739±4342*	3/5	4/5	4/5
GSH-OEt(+) anti-Fas	0	26±10	32±8	25±9	5/5	5/5	5/5
GSH-OEt(+) anti-Fas	4	671±106	431±96	398±119	5/5	5/5	5/5
GSH-OEt(+) anti-Fas	8	2621±766	1832±805	2798±468	5/5	5/5	5/5
GSH-OEt(+) anti-Fas	12	4944±563	3456±934	4878±889	5/5	5/5	5/5

Anti-Fas antibody (Jo-2, 2 μg/mouse) was administered intraperitoneally as a mixture in 0.2 ml of pyrogen-free saline to 12-week-old Nrf2-deficient and wild-type (BSO-treated and -untreated) mice. At 0, 4, 8, and 12 h after injection, blood was collected and serum ALT activities were determined as indices of hepatotoxicity using an automated analyser (DRY-CHEM 3500; Fuji Film). GSH-OEt (20 mg/mouse) was injected intravenously 2 h before anti-Fas antibody injection to increase the intracellular GSH level. Results are expressed as mean±s.d. for three to five mice. The survival rate indicates the number of survived/all mice. *Significantly different from wild-type (BSO-untreated) mice ($P<0.05$)

Table 2 Hepatotoxicity and lethal effect in Nrf2-deficient and BSO-treated mice induced by TNF-α

		ALT (IU/l)			*Survival rate (survived/all)*		
Treatment	*Time (h)*	*Nrf2 deficient*	*Wild type*	*BSO-treated wild type*	*Nrf2 deficient*	*Wild type*	*BSO-treated wild type*
GSH-OEt(−) TNF-α	0	31±8	41±8	42±4	5/5	5/5	5/5
GSH-OEt(−) TNF-α	4	942±301 *	235±104	873±276*	5/5	5/5	5/5
GSH-OEt(−) TNF-α	8	8207±1431*	1642±815	5642±2142*	4/5	5/5	4/5
GSH-OEt(−) TNF-α	12	8732±4413*	1901±1403	6739±3732*	3/5	4/5	4/5
GSH-OEt(+) TNF-α	0	25±9	37±11	33±7	5/5	5/5	5/5
GSH-OEt(+) TNF-α	4	363±182	212±84	375±130	5/5	5/5	5/5
GSH-OEt(+) TNF-α	8	1837±765	898±562	1098±501	5/5	5/5	5/5
GSH-OEt(+) TNF-α	12	2247±1989	1267±1217	2878±842	5/5	5/5	5/5

TNF-α (0.5 μg) (obtained from BD Bioscience) was administered intraperitoneally as a mixture in 0.2 ml of pyrogen-free saline to 12-week-old Nrf2-deficient and wild-type (BSO-treated and -untreated) mice. D-Galactosamine hydrochloride (GalN) (obtained from Nacalai Tesque) was preinjected intravenously to increase the susceptibility of mice to hepatotoxicity 30 min before TNF-α injection. GSH-OEt (20 mg/mouse) was injected intravenously 2 h before TNF-α injection to assess the importance of the intracellular GSH level. At 0, 4, 8, and 12 h after injection, blood was collected and serum ALT activities were determined. Results are shown as mean±s.d. for three to five mice. The survival rate indicates number of survived/all mice. *Significantly different from wild-type mice ($P<0.05$)

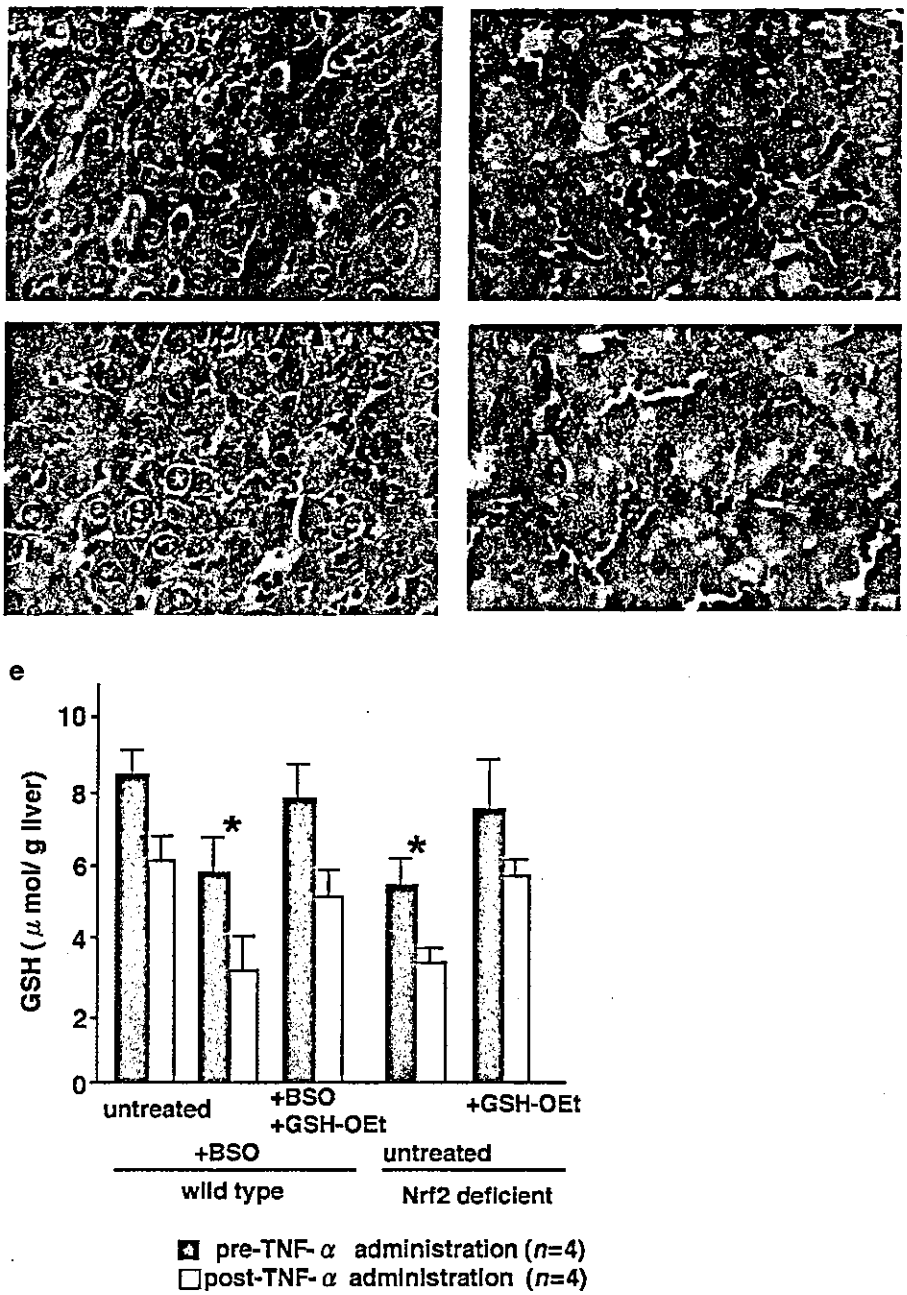

Figure 2 Nrf2 deficiency enhanced TNF-α-mediated apoptosis and GSH-OEt rescued Nrf2-deficient mice from TNF-α-mediated apoptosis. Mice were killed 12 h after TNF-α (0.5 μg) injection. GalN was preinjected intravenously 30 min before TNF-α injection. GSH-OEt (20 mg) was injected 2 h before TNF-α administration to increase intracellular glutathione levels. The liver was excised, fixed with 10% buffered formalin, sectioned at a thickness of 5 μm, and stained with hematoxylin and eosin for light microscopic examination. (a) Liver section of wild-type mouse: a few apoptotic hepatocytes exhibit apoptotic nuclei. (b) Nrf2-deficient mouse: numerous apoptotic hepatocytes were observed (arrows indicate apoptotic nuclei). (c) Nrf2-deficient mouse with GSH-OEt administration: apoptotic cells were decreased by the addition of GSH-OEt. (d) BSO-treated wild-type mouse: numerous apoptotic hepatocytes were observed as seen in Nrf2-deficient mouse (arrows also indicate apoptotic nuclei). (e) GSH levels of livers were examined pre- and post-TNF-α administration. The total GSH level was measured in homogenized liver samples. The GSH level of Nrf2-deficient livers was significantly reduced compared to wild type being decreased to almost the same level as that of BSO-treated livers. GSH-OEt addition increased the GSH levels of Nrf2-deficient and BSO-treated livers to almost the same level as that of Nrf2 wild-type liver. *Significant difference from untreated wild-type livers ($P<0.05$)

low level of intracellular GSH might be the cause of the enhancement. To confirm this theory, we investigated the effect of chronically treating the mice with BSO. Serum ALT activity after Fas stimulation was significantly increased in BSO-treated wild-type mice compared to untreated wild-type mice ($P<0.05$) (Table 1). The addition of GSH-OEt cancelled the enhancement of Fas-induced fulminant hepatitis in BSO-treated mice. These results suggest that a low level of intracellular GSH could be the cause of the enhancement *in vivo*.

Fas and TNF-RI share homology at their cytoplasmic death domain, a region necessary for apoptotic signaling (Schulze-Osthoff *et al.*, 1998). D-Galactosamine (GalN) is well known to increase the susceptibility of mice to hepatotoxicity and the lethal effects of TNF-α. Therefore, the effect of TNF-α on hepatocellular apoptosis in GalN-sensitized Nrf2-deficient mice was examined. TNF-α (0.5 μg/mice) was administered intraperitoneally to GalN-sensitized Nrf2-deficient and wild-type mice. The result showed that serum ALT activity after TNF-α administration was significantly increased in Nrf2-deficient mice compared to wild-type mice. The mean ALT activity in the sera from Nrf2-deficient mice was 8732±4413 IU/l at 12 h after induction (Table 2). On the other hand, the ALT activity of wild-type mice was less than 2000 IU/l when taken at the same time point. This represents a fourfold difference of ALT activity between these two groups. GSH-OEt addition decreased the ALT activity in Nrf2-deficient mice to almost the same level as that of wild-type mice. To investigate the influence of GSH depletion, we examined wild-type mice chronically treated with BSO. Serum ALT activity after TNF-α stimulation was significantly increased in BSO-treated wild-type mice compared to untreated wild-type mice ($P<0.05$) (Table 2). The addition of GSH-OEt decreased the enhancement of TNF-α-induced fulminant hepatitis in BSO-treated wild-type mice. This result suggested that a low level of intracellular GSH would be the cause of the enhanced TNF-α-mediated apoptosis.

Histopathological examination revealed that the number of apoptotic hepatocytes was increased in Nrf2-deficient mice compared to wild-type mice (Figure 2). Massive hepatocyte apoptosis, as judged by the frequent appearance of nuclear fragmentation and a hyperchromatic nuclear membrane, was observed in Nrf2-deficient mice (Figure 2b). Further major pathological signs included diffuse congestive hemorrhagic foci (Figure 2b). In contrast, liver specimens from a comparable area taken from mice injected with GSH-OEt before TNF-α administration showed a morphology (Figure 2c) that was indiscernible from that of wild-type mice (Figure 2a). BSO-treated wild-type mice revealed massive hepatocyte apoptosis by TNF-α administration as well as Nrf2-deficient mice (Figure 2d). The administration of GSH-OEt to BSO-treated wild-type mice re-established the sensitivity of TNF-α-mediated apoptosis to the level of wild-type mice as judged by histological appearance (data not shown). The histological analyses also support the fact that Nrf2 deficiency enhances the sensitivity of TNF-α-mediated apoptosis as a consequence of GSH depletion.

To confirm the effect of GSH on TNF-α-mediated apoptosis *in vivo*, we determined the total liver GSH levels (Figure 2e). Mice were killed 4 h after TNF-α and GalN administration. Livers were homogenized and the total GSH levels were measured. The GSH level of Nrf2-deficient livers was decreased to almost the same level as that of BSO-treated wild-type livers. GSH-OEt addition increased the GSH levels of Nrf2-deficient and BSO-treated wild-type livers to almost the same level as that of Nrf2 wild-type livers. These results suggest that chronic GSH depletion can enhance TNF-α-mediated apoptosis *in vivo*.

An accumulating number of reports describe the relationship between Nrf2 and various kinds of stresses. Cho *et al.* (2002) reported that Nrf2 had a key protective role during hyperoxic lung injury. Enomoto *et al.* (2001) and Chan *et al.* (2001) clearly demonstrated an enhanced susceptibility to acetaminophen in Nrf2-deficient mice. We also reported that Nrf2 female mice developed autoimmune glomerulonephritis probably due to susceptibility to oxidative stress (Yoh *et al.*, 2001). In addition, Ramos-Gomez *et al.* (2001) showed that Nrf2 was central to the constitutive and inducible expression of phase two enzymes *in vivo* and dramatically influences susceptibility to carcinogens. However, few studies reported the relationship between Nrf2 and apoptosis. This study is the first report describing Nrf2 as regulating the sensitivity of death receptor signals through intracellular glutathione levels *in vivo*. The inhibition of the death signal is a novel role of Nrf2. Possibly, the observed enhancement in death signals caused by a deficiency in Nrf2 is a safety mechanism to eliminate cells that have accumulated damage as a consequence of an inadequate stress response. Further analyses must be performed to explore the relationship between apoptotic regulation by Nrf2 and various stresses including diseases.

Acknowledgements

This work was supported in part by Grants-in-Aid from the Ministry of Education, Science, Sports and Culture, the Japanese Society for Promotion of Sciences (RFTF), Core Research for Evolutional Sciences and Technology (CREST), and Program for Promotion of Basic Research Activities for Innovative Biosciences (PROBRAIN). We thank Vincent Kelly (Banyu Pharmaceutical Co., Ltd) for their help and discussion and N Kaneko (University of Tsukuba) for their excellent assistance.

References

Anderson ME. (1997). *Adv. Pharmacol.*, **38**, 65–78.

Chan JY and Kwong M. (2000). *Biochim. Biophys. Acta*, **1517**, 19–26.

Chan K, Han XD and Kan YW. (2001). *Proc. Natl. Acad. Sci. USA*, **98**, 4611–4616.

Chen TS, Richie JP, Nagasawa HT and Lang CA. (2001). *Mech. Ageing Dev.*, **120**, 127–139.

Chiba T, Takahashi S, Sato N, Ishii S and Kikuchi K. (1996). *Eur. J. Immunol.*, **26**, 1164–1169.

Cho HY, Jedlicka AE, Reddy SP, Kensler TW, Yamamoto M, Zhang LY and Kleeberger SR. (2002). *Am. J. Respir. Cell Mol. Biol.*, **26**, 175–182.

Colell A, Garcia-Ruiz C, Miranda M, Ardite E, Mari M, Morales A, Corrales F, Kaplowitz N and Fernandez-Checa JC. (1998). *Gastroenterology*, **115**, 1541–1551.

Droge W, Schulze-Osthoff K, Mihm S, Galter D, Schenk H, Eck HP, Roth S and Gmunder H. (1994). *FASEB J.*, **8**, 1131–1138.

Enomoto A, Itoh K, Nagayoshi E, Haruta J, Kimura T, O'Connor T, Harada T and Yamamoto M. (2001). *Toxicol. Sci.*, **59**, 169–177.
Favreau LV and Pickett CB. (1991). *J. Biol. Chem.*, **266**, 4556–4561.
Galle PR, Hofmann WJ, Walczak H, Schaller H, Otto G, Stremmel W, Krammer PH and Runkel L. (1995). *J. Exp. Med.*, **182**, 1223–1230.
Hall AG. (1999). *Eur. J. Clin. Invest.*, **29**, 238–245.
Haouzi D, Lekehal M, Tinel M, Vadrot N, Caussanel L, Letteron P, Moreau A, Feldmann G, Fau D and Pessayre D. (2001). *Hepatology*, **33**, 1181–1188.
Hentze H, Gantner F, Kolb SA and Wendel A. (2000). *Am. J. Pathol.*, **156**, 2045–2056.
Hentze H, Kunstle G, Volbracht C, Ertel W and Wendel A. (1999). *Hepatology*, **30**, 177–185.
Hirata H, Takahashi A, Kobayashi S, Yonehara S, Sawai H, Okazaki T, Yamamoto K and Sasada M. (1998). *J. Exp. Med.*, **187**, 587–600.
Ishii T, Itoh K, Takahashi S, Sato H, Yanagawa T, Katoh Y, Bannai S and Yamamoto M. (2000). *J. Biol. Chem.*, **275**, 16023–16029.
Itoh K, Chiba T, Takahashi S, Ishii T, Igarashi K, Katoh Y, Oyake T, Hayashi N, Satoh K, Hatayama I, Yamamoto M and Nabeshima Y. (1997). *Biochem. Biophys. Res. Commun.*, **236**, 313–322.
Itoh K, Igarashi K, Hayashi N, Nishizawa M and Yamamoto M. (1995). *Mol. Cell. Biol.*, **15**, 4184–4193.
Itoh K, Ishii T, Wakabayashi N and Yamamoto M. (1999). *Free Radic. Res.*, **31**, 319–324.
Jones TW, Thor H and Orrenius S. (1986). *Arch. Toxicol.*, **9** (Suppl.), 259–271.
Kotlo KU, Yehiely F, Efimova E, Harasty H, Hesabi B, Shchors K, Einat P, Rozen A, Berent E and Deiss LP. (2003). *Oncogene*, **22**, 797–806.
Leist M, Gantner F, Kunstle G, Bohlinger I, Tiegs G, Bluethmann H and Wendel A. (1996). *Mol. Med.*, **2**, 109–124.
Medema JP, Scaffidi C, Kischkel FC, Shevchenko A, Mann M, Krammer PH and Peter ME. (1997). *EMBO J.*, **16**, 2794–2804.
Meister A. (1992). *Biochem. Pharmacol.*, **44**, 1905–1915.
Moi P, Chan K, Asunis I, Cao A and Kan YW. (1994). *Proc. Natl. Acad. Sci. USA*, **91**, 9926–9930.
Nagata S. (1997). *Cell*, **88**, 355–365.
Ogasawara J, Watanabe-Fukunaga R, Adachi M, Matsuzawa A, Kasugai T, Kitamura Y, Itoh N, Suda T and Nagata S. (1993). *Nature*, **364**, 806–809.
Prestera T, Talalay P, Alam J, Ahn YI, Lee PJ and Choi AM. (1995). *Mol. Med.*, **1**, 827–837.
Rahman I, Mulier B, Gilmour PS, Watchorn T, Donaldson K, Jeffery PK and MacNee W. (2001). *Biochem. Pharmacol.*, **62**, 787–794.
Ramos-Gomez M, Kwak MK, Dolan PM, Itoh K, Yamamoto M, Talalay P and Kensler TW. (2001). *Proc. Natl. Acad. Sci. USA*, **98**, 3410–3415.
Rushmore TH, King RG, Paulson KE and Pickett CB. (1990). *Proc. Natl. Acad. Sci. USA*, **87**, 3826–3830.
Srivastava SK, Xia H, Pal A, Hu X, Guo J and Singh SV. (2000). *Cancer Lett.*, **153**, 35–39.
Schulze-Osthoff K, Ferrari D, Los M, Wesselborg S and Peter ME. (1998). *Eur. J. Biochem.*, **254**, 439–459.
Thronberry NA and Lazebnik Y. (1998). *Science*, **281**, 1312–1316.
Uhlig S and Wendel A. (1992). *Life Sci.*, **51**, 1083–1094.
Widmann C, Gibson S and Johnson GL. (1998). *J. Biol. Chem.*, **273**, 7141–7147.
Xu Y, Jones BE, Neufeld DS and Czaja MJ. (1998). *Gastroenterology*, **115**, 1229–1237.
Yoh K, Itoh K, Enomoto A, Hirayama A, Yamaguchi N, Kobayashi M, Morito N, Koyama A, Yamamoto M and Takahashi S. (2001). *Kidney Int.*, **60**, 1343–1353.
Zhivotovsky B, Burgess DH, Vanags D M and Orrenius S. (1997). *Biochem. Biophys. Res. Commun.*, **230**, 481–488.

nature genetics

Keap1-null mutation leads to postnatal lethality due to constitutive Nrf2 activation

Nobunao Wakabayashi[1], Ken Itoh[1,2], Junko Wakabayashi[1], Hozumi Motohashi[1], Shuhei Noda[1], Satoru Takahashi[3], Sumihisa Imakado[4], Tomoe Kotsuji[4], Fujio Otsuka[4], Dennis R Roop[5], Takanori Harada[6], James Douglas Engel[7] & Masayuki Yamamoto[1–3]

Transcription factor Nrf2 (encoded by *Nfe2l2*) regulates a battery of detoxifying and antioxidant genes, and Keap1 represses Nrf2 function. When we ablated *Keap1*, Keap1-deficient mice died postnatally, probably from malnutrition resulting from hyperkeratosis in the esophagus and forestomach. Nrf2 activity affects the expression levels of several squamous epithelial genes. Biochemical data show that, without Keap1, Nrf2 constitutively accumulates in the nucleus to stimulate transcription of cytoprotective genes. Breeding to Nrf2-deficient mice reversed the phenotypic Keap1 deficiencies. These experiments show that Keap1 acts upstream of Nrf2 in the cellular response to oxidative and xenobiotic stress.

Transcription factor Nrf2/ECH belongs to the cap-n-collar family of activators that shares a highly conserved basic region–leucine zipper structure[1–3]. Nrf2 forms heterodimers with the small Maf proteins[3,4] and binds to the antioxidant responsive elements (AREs) or electrophile responsive elements of target genes. We previously showed through gene targeting that Nrf2 regulates a battery of genes encoding drug metabolizing enzymes and antioxidant proteins[5]. In efforts to elucidate the pathway leading to oxidative and xenobiotic stress response through Nrf2, Keap1 (Kelch-like ECH associating protein 1) was identified as a potential effector of Nrf2 (ref. 6). Several lines of evidence suggested that Nrf2 and Keap1 might have a vital role in regulating cellular defenses against a variety of environmental insults, for example, in the electrophile counterattack response[7], acetaminophen intoxication[8], chemical carcinogenesis[9] and diesel exhaust inhalation[10].

Keap1 is composed of two distinguishable motifs: the Kelch (or double glycine repeat) domain[11] and a BTB/POZ domain[12]. The BTB domain has been shown to form homomeric and heteromeric multimers[13], but the BTB function of Keap1 has not been fully elucidated[14]. The Kelch domain is named after the *Drosophila* egg-chamber regulatory protein Kelch[15–18]. Through the Kelch domain, Keap1 interacts with and sequesters Nrf2 in the cytoplasm through association with the actin cytoskeleton.

We previously reported that Keap1 is a key regulator of Nrf2 function[6] and proposed a molecular mechanism by which the two proteins could collaborate to regulate transcription. In this model, Nrf2 binds to the Kelch domain of Keap1 and is thereby retained in the cytoplasm under normal physiological conditions. The model also proposes that when cells encounter oxidative or xenobiotic stress, Nrf2 can be released from Keap1 (and the actin cytoskeleton), allowing it to rapidly traverse to the nucleus[6,7].

To test the main tenets of this model for Nrf2 regulation by Keap1, we generated mice bearing a targeted mutation in *Keap1*. Homozygous *Keap1* mutant newborns were normal but all died unexpectedly within three weeks after birth. The pups had severe growth retardation and a gross scaling phenotype that became evident by 5 d after birth. Detailed postmortem analysis detected severe hyperkeratosis in the esophagus and forestomach of these mutants. The hyperkeratotic lesions constricted the esophagus and cardia, obstructing milk flow. Thus, postnatal death was probably due to starvation. We also found that the Nrf2-Keap1 pathway regulates a subset of genes induced in squamous cell epithelia in response to mechanical stress. All of the Keap1-dependent phenotypes were reversed in *Keap1-Nrf2* double mutants, indicating that the Keap1 deficiency allowed Nrf2 to constitutively accumulate in the nucleus. We showed that Nrf2 accumulated in the nuclei of homozygous *Keap1*-mutant cells and that constitutive expression of Nrf2 target genes was markedly increased. These results directly support the hypothesis that Nrf2-Keap1 homeostasis is a regulatory nexus controlling the cellular response not only to oxidative and xenobiotic stress but also potentially to stress induced by mechanical injury.

RESULTS

Targeted mutation of *Keap1*

To examine the contribution of Keap1 to the postulated regulation of Nrf2 function *in vivo*, we disrupted the *Keap1* gene. We replaced

[1]Center for Tsukuba Advanced Research Alliance, [2]ERATO-JST, [3]Institutes of Basic Medical Sciences and [4]Clinical Medical Sciences, University of Tsukuba, 1-1-1 Tennoudai, Tsukuba 305-8577, Japan. [5]Departments of Molecular and Cellular Biology and Dermatology, Baylor College of Medicine, One Baylor Plaza, Houston, Texas 77030, USA. [6]The Institute of Environmental Toxicology 4321 Uchimoriya-cho, Mitsukaido-shi, Ibaraki 303-0043, Japan. [7]Department of Cell and Developmental Biology, University of Michigan Medical School, 1335 Catherine, Ann Arbor, Michigan 48109, USA. Correspondence should be addressed to M.Y. (masi@tara.tsukuba.ac.jp).

Published online 28 September 2003; doi:10.1038/ng1248

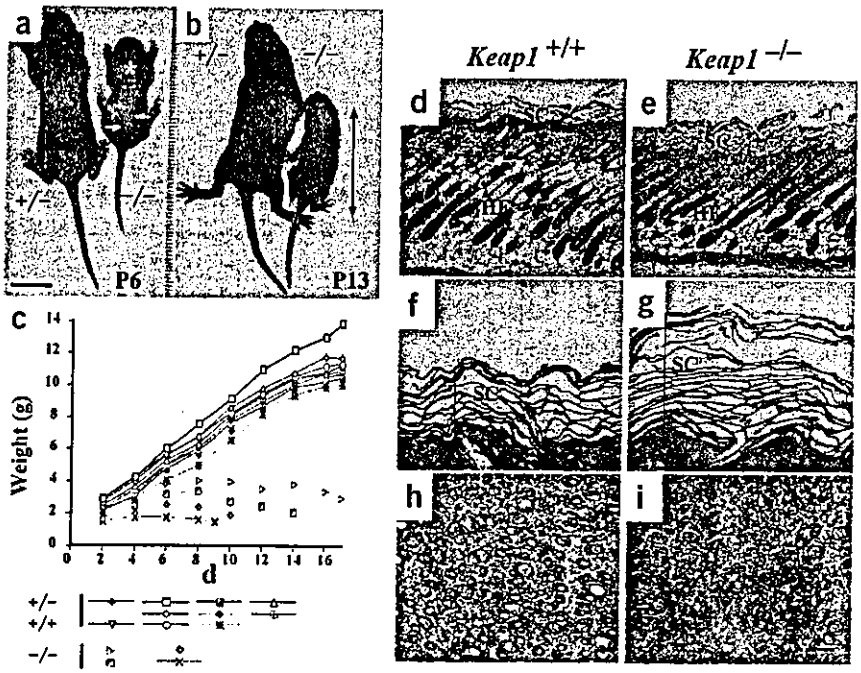

Figure 1 Growth retardation and skin abnormalities in Keap1-deficient mice. (**a**) A P6 *Keap1* homozygous mutant mouse (–/–) is shown alongside a *Keap1* heterozygous (+/–) littermate. The homozygous mutant mouse has fine scales (yellow arrows) and topical skin disorder (asterisk). Scale bar = 1 cm. (**b**) Appearance of P13 $Keap1^{+/-}$ and $Keap1^{-/-}$ female littermates. Arrow = 3 cm. (**c**) Growth curves for *Keap1* mutant and wild-type littermate mice. Genotypes (shown below graph) were determined at the end of the observation period. (**d–i**) Skin sections of wild-type (**d,f,h**) or $Keap1^{-/-}$ (**e,g,i**) mice. Male mice (P6) from a single litter were analyzed. Identical low-power (**d,e,h,i**) or high-power (**f,g**) magnifications of ventral epidermal thin sections are depicted. Note the thickening of the cornified skin (SC, stratum corneum) layer. HF, hair follicles. Scale bars = 100 μm (**d,e,h,i**) or 25 μm (**f,g**).

residues 8–204 of Keap1 with a nuclear localization signal (NLS)-tagged *lacZ* gene (**Supplementary Fig. 1** online). We established two independent lines of mice bearing the *Keap1* mutation, whose phenotypes were identical. We verified homologous recombination at the gene-targeted locus in embryonic stem (ES) cells and mutant mice by Southern-blot hybridization. We used probes specific for the 5′ and 3′ ends of the targeting vector to detect genomic DNA fragment differences in *Eco*RI- or *Sac*I-digested genomic DNA. In ES cells and genomic DNA from mutant tails, we detected the predicted sizes of mutant DNA fragments (**Supplementary Fig. 1** online).

The level of *Keap1* mRNA in $Keap1^{+/-}$ mouse embryonic fibroblasts (MEFs) was approximately half of that detected in wild-type MEFs, but no *Keap1* mRNA was detected in $Keap1^{-/-}$ MEFs (**Supplementary Fig. 1** online). Immunoblotting with an antibody to β-galactosidase showed that NLS-LacZ was roughly twice as abundant in $Keap1^{-/-}$ mice as in $Keap1^{+/-}$ mice (**Supplementary Fig. 1** online). Thus, the *Keap1* gene was effectively disrupted.

Keap1-deficient mice survive until weaning

We routinely recovered $Keap1^{-/-}$ mutant pups from $Keap1^{+/-}$ intercrosses. Their size and behavior at birth was indistinguishable from those of wild-type and heterozygous littermates. Beginning around postnatal day (P) 4, however, we observed severe growth retardation of the $Keap1^{-/-}$ mice (**Fig. 1a,b**), despite their apparently normal suckling ability. In addition, scales began to appear at P5 and covered the body of $Keap1^{-/-}$ mice. None of the $Keap1^{-/-}$ mutants survived beyond P21 (**Fig. 1c**), but all died of gradually progressive asthenia. Necropsy showed that the size of each organ of $Keap1^{-/-}$ mice was proportional to the body dimensions. We examined histologically various organs of $Keap1^{-/-}$ pups at P2–P14 but noted no other morphological abnormality (data not shown), except in the esophagus and forestomach (see below). We carried out laboratory examinations of P7 mice, which showed that serum levels of sodium, potassium, glutamic-oxaloacetic transaminase, blood urea nitrogen and amylase of *Keap1*-null mice were statistically indistinguishable from those of wild-type littermates.

Hyperkeratosis in esophagus and forestomach

To investigate the scaling skin phenotype of Keap1-deficient mice at P5 and P6, we prepared longitudinal (**Fig. 1d–g**) or horizontal sections (**Fig. 1h,i**) of skin from these mice. In comparison to skin from their wild-type littermates, the stratum corneum was noticeably thicker and sometimes looked less compact in $Keap1^{-/-}$ mice (**Fig. 1d–g**). But *Keap1*-null mice had similar numbers of hair follicles as did wild-type mice (**Fig. 1h,i**); P6–P9 wild-type, $Keap1^{+/-}$ and $Keap1^{-/-}$ mice had 214 ± 21, 235 ± 30 and 166 ± 31 hair follicles per mm^2, respectively ($n = 6$ per genotype). We also examined the presence of squamous cell differentiation markers, keratin K1, filaggrin and loricrin, by immunostaining. The levels of suprabasal K1 and of filaggrin did not differ significantly between $Keap1^{-/-}$ and wild-type

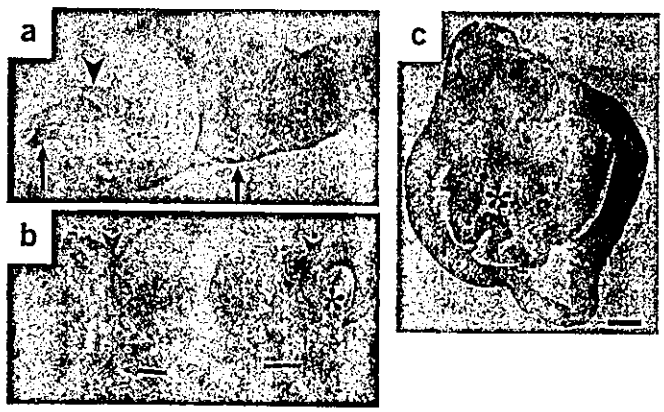

Figure 2 Macroscopic observation of stomachs of Keap1-deficient mice. (**a,b**) External and internal appearance of the stomachs of P16 wild-type (**a**) or $Keap1^{-/-}$ (**b**) male littermates. Arrowheads and arrows indicate the cardiac part and the pyloric segment of the stomach, respectively. Asterisks indicate solid keratinous mass. (**c**) A thin horizontal section through the stomach of a P16 *Keap1* homozygous mutant male at the cardiac part and limiting ridge level. An arrowhead indicates the cardiac part, and an asterisk indicates a solid keratinous mass. Scale bar = 500 μm (**c**).

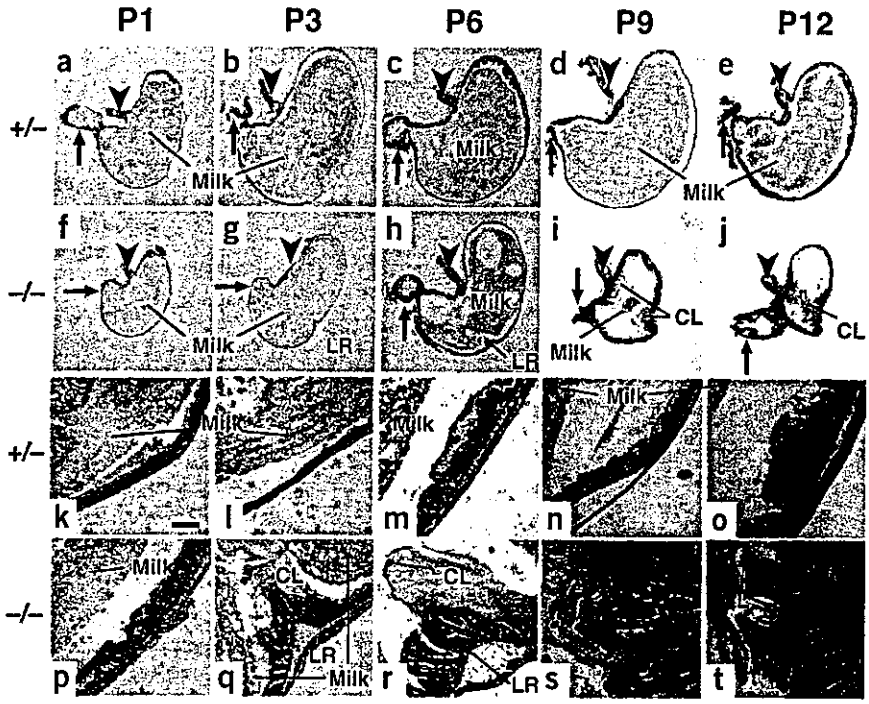

Figure 3 Histological analysis of stomachs of Keap1-deficient mice during development. (**a–j**) Sagittal sections of the whole stomachs of *Keap1*$^{+/-}$ (**a–e**) and *Keap1*$^{-/-}$ (**f–j**) mice. Arrowheads and arrows indicate the cardiac part and the pyloric segment of the stomach, respectively. Note the accumulation of cornified layers (CL) in Keap1-deficient mice at P9 and P12. (**k–t**) High-power magnification of the limiting ridge (LR) regions of *Keap1*$^{+/-}$ (**k–o**) and *Keap1*$^{-/-}$ (**p–t**) mouse stomachs. Epithelial cornification of the forestomach of *Keap1*$^{-/-}$ (**q–t**) mouse is evident compared with the forestomach of the wild-type (**l–o**) mouse. Scale bar = 100 μm (**k–t**).

mice, but the terminal differentiation marker loricrin was more abundant in the skin of *Keap1*$^{-/-}$ mice (data not shown).

The stomachs of *Keap1*-null mutant pups were much smaller than those of wild-type pups (**Fig. 2a**). Consistent with the skin abnormality, but far more acute, we detected multiple cornified layers on the inner wall of the esophagus and forestomach of *Keap1* mutants and a large mass in the lumen (**Fig. 2b**), which was palpable from outside of the gastric wall. This phenotype was fully penetrant.

Thin sectioning of the esophagus and forestomach showed that the mass was composed of many layers of cornified cells (**Fig. 2c**). In the P1–P6 stage, the stomachs of control and Keap1-deficient mice were filled with milk, and the hyperkeratotic phenotype was not obvious (**Fig. 3a–c,f–h**). But we observed a thickened cornified layer in the forestomach of Keap1-deficient mice by P9 (**Fig. 3d,i**). At more advanced stages (**Fig. 3e,j**), the thickened cornified layer detached from the forestomach mucosa and formed a multilayered keratinous mass that occupied the gastric lumen. The detached area of the mucosa developed severe ulceration accompanied by inflammatory cell infiltration. In the glandular portion of the stomach, the mucosa was relatively intact, although we observed inflammation and detachment of epithelium at advanced stages.

Under higher magnification, the thickening of the cornified layer was apparent as early as P3 in the region adjacent to the limiting ridge (**Fig. 3k,l,p,q**). The thickened stratum corneum expanded in the forestomach side of the limiting ridge by P6 (**Fig. 3m,r**), and the expansion proceeded severely thereafter (**Fig. 3n,o,s,t**). These results indicate that the Keap1 deficiency leads to abnormal cornification, which results in a huge mass in the cardiac part. We suspect that gastric obstruction and reduced compliance due to excessive hyperkeratosis may be the primary cause of the premature death of *Keap1* mutant mice.

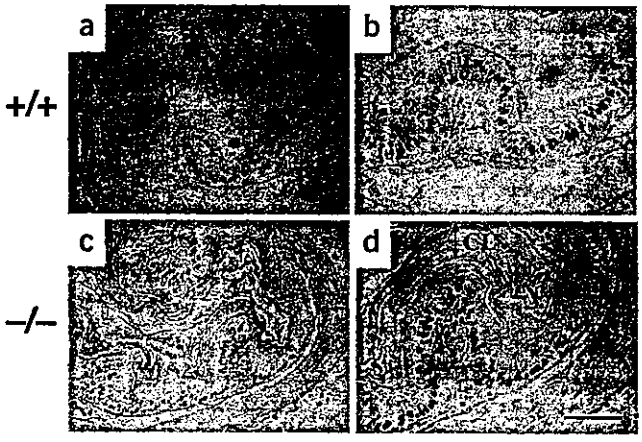

Figure 4 Squamous cell proliferation in esophagus of *Keap1* mutant mice. (**a–d**) Immunohistochemical detection of PCNA. (**a,b**) Wild-type esophageal section. (**c,d**) *Keap1*$^{-/-}$ esophageal section. Panels **b** and **d** are higher magnifications of **a** and **c**, respectively. The thickened cornified layer (CL) of the *Keap1*$^{-/-}$ mouse is indicated with a double-ended arrow. Scale bars = 100 μm (**a,c**) and 50 μm (**b,d**).

Induction of keratin K1, K6 and loricrin

When we detected proliferating cells in the esophageal epithelium with an antibody against proliferating cell nuclear antigen (PCNA), the ratio of immature squamous cells to total squamous cells was not substantially higher in *Keap1*-null mice compared with normal littermates (**Fig. 4**). This result indicates that the hyperkeratosis did not accompany the outgrowth of the esophageal epithelium.

To determine if any changes could be detected in the expression of specific squamous cell differentiation markers, we carried out immunohistochemical analysis on esophageal samples. Bright-field images of wild-type and *Keap1*-null mutant mouse esophagi (**Fig. 5a,b**) showed considerable variation in the level of expression of several proteins, well characterized as differentiation and proliferation markers of epidermal cells. Expression of the suprabasal cytokeratin K1 (**Fig. 5c,d**) and the terminal differentiation marker loricrin (**Fig. 5e,f**) in the homozygous *Keap1* mutant esophagus was much higher than in esophagi of wild-type littermates. In contrast, the expression of another suprabasal cytokeratin, K13, was slightly diminished (**Fig. 5g,h**) and that of basal cytokeratin K14 (**Fig. 5i,j**) was unchanged in *Keap1*$^{-/-}$ mutants relative to wild-type littermates. Double staining with antibodies to loricrin and K14 confirmed that loricrin production was induced and that K14 abundance was unchanged in the esophagi of Keap1-deficient pups (**Fig. 5k,l**).

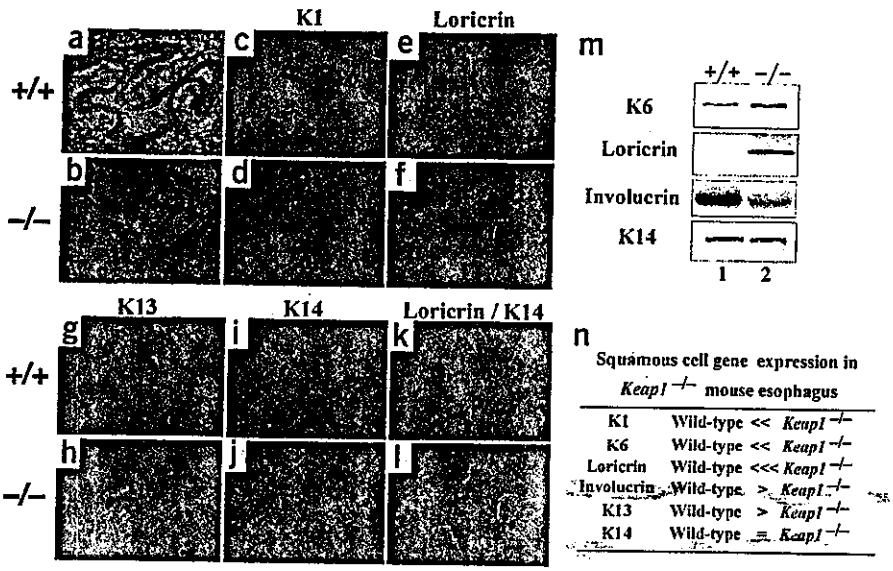

Figure 5 Aberrant expression of squamous cell genes in Keap1-deficient mice. (a–l) Immunohistochemical detection of squamous cell genes in *Keap1*-null and wild-type esophagi. Specimens were taken from esophagi between the cardiac segment and pharynx of wild-type or *Keap1*$^{-/-}$ mice. (a,b) Bright-field images of sections from wild-type and *Keap1* homozygous mutant esophagi, respectively. A series of serial sections (7 μm) was treated with antibodies to cytokeratin K1 (c,d), loricrin (e,f), K13 (g,h) or K14 (i,j). (k,l) Double immunostaining with antibodies to both K14 (red) and loricrin (green). (m) Immunoblotting analysis of K6, loricrin, involucrin and K14 in the *Keap1* homozygous mutant mouse. Proteins extracted from the middle part of the esophagus of wild-type (+/+) or *Keap1*-null mutant (−/−) mice were subjected to immunoblotting analyses. (n) A summary of squamous cell gene expression changes in Keap1-deficient mice as compared to their wild-type littermates.

We quantified these changes in squamous cell differentiation markers more thoroughly by immunoblot analysis using antibodies to K6, loricrin, involucrin and K14. Whereas keratin K14 levels were essentially unaffected by the *Keap1* mutation, loricrin and keratin K6 (ref. 19) were markedly induced, and involucrin levels were diminished, in *Keap1* mutant esophagi (Fig. 5m,n). These results suggested that the synthesis of specific squamous cell differentiation products is under the negative control of Keap1 and that the Keap1 deficiency results in hyperkeratosis.

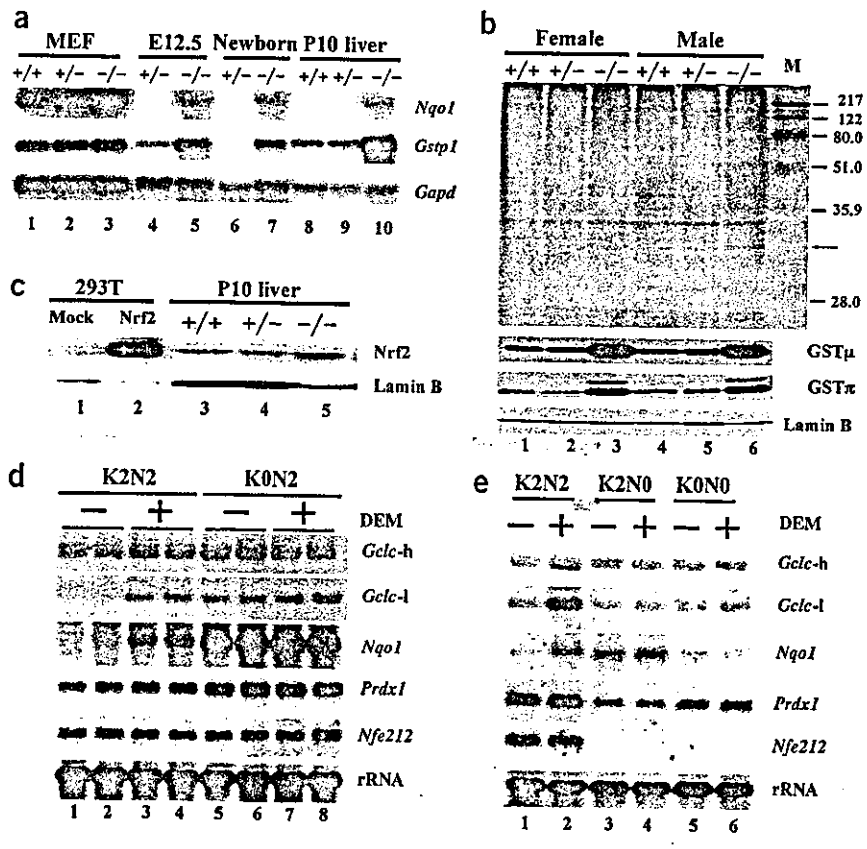

Figure 6 Drug metabolizing enzymes and antioxidant proteins are constitutively expressed in Keap1-deficient mice and cells. (a) RNA blotting analysis of *Nqo1* and *Gstp1* in the livers of wild-type (+/+), *Keap1* heterozygous (+/−) or homozygous mutant (−/−) mice. RNA samples from MEFs (lanes 1–3), E12.5 embryo livers (lanes 4,5), P0 mouse livers (lanes 6,7) or P10 mouse livers (lanes 8–10) were examined. MEFs and livers were taken from wild-type (lanes 1,8), *Keap1*$^{+/-}$ (lanes 2,4,6,9) or *Keap1*$^{-/-}$ (lanes 3,5,7,10) mice. *Gapd* was used as an internal control (bottom panel). (b) Immunoblotting of GSTμ and GSTπ recovered from the livers of P10 wild-type, *Keap1* heterozygous or homozygous mutant mice. The top panel shows gel electrophoresis patterns of total protein extracted from the livers of male and female P10 wild-type (lanes 1,4), *Keap1*$^{+/-}$ (lanes 2,5) or *Keap1*$^{-/-}$ (lanes 3,6) mice. The increase in GST proteins can be visualized in the Coomassie blue–stained gel (lanes 3,6; arrow). Expression of GSTμ and GSTπ in the liver was analyzed immunochemically with specific antibodies (two middle panels). Lamin B was used as an internal control (bottom panel). M, molecular weight marker. (c) Nrf2 expression in P10 liver nuclei from wild-type, *Keap1*$^{+/-}$ or *Keap1*$^{-/-}$ mice. Total nuclear proteins from 293T cells transfected with either pEF-BOS (mock; lane 1) or pEFmNrf2 (lane 2) expression vectors were used as standards for Nrf2 detection. Nuclear extracts were prepared from the livers of wild-type (lane 3), *Keap1*$^{+/-}$ (lane 4) or *Keap1*$^{-/-}$ (lane 5) mice. Lamin B was used as an internal control. (d) RNA-blot analysis of cytoprotective enzymes in *Keap1* mutant MEFs. MEFs were prepared from wild-type (K2N2; lanes 1–4) or *Keap1* mutant (K0N2; lanes 5–8) embryos and cultured with (lanes 3,4,7,8) or without (lanes 1,2,5,6) DEM. (e) RNA-blot analysis of cytoprotective enzymes in *Keap1-Nfe2l2* compound mutant MEFs. MEFs were prepared from wild-type (K2N2; lanes 1,2), *Nfe2l2* mutant (K2N0; lanes 3,4) or *Keap1-Nfe2l2* compound mutant (K0N0; lanes 5,6) embryos and cultured with (lanes 2,4,6) or without (lanes 1,3,5) DEM. (d,e) Total RNAs were probed with cytoprotective enzyme cDNAs and *Nfe2l2* cDNA.

We next investigated whether the effect of Nrf2 on expression of squamous differentiation genes was direct or indirect. In searching the mouse genome database, we found ARE motifs in the genes encoding loricrin and K6a. To test whether the loricrin ARE at −823 (ref. 20) directly transduces Nrf2 activity, we prepared luciferase reporters and transfected them into primary normal human epidermal keratinocytes expressing loricrin. Cotransfection of an Nrf2 expression plasmid induced the loricrin reporter construct approximately fivefold, but this increase was eliminated when the ARE sequence was mutated (data not shown). Thus, induction of loricrin in *Keap1*$^{-/-}$ mutants is probably a direct effect of constitutive Nrf2 activity. Another squamous differentiation gene containing an ARE is that encoding keratin K6a[21]. We linked one copy of this ARE to the thymidine kinase promoter directing expression of luciferase. We observed induction of Nrf2 and repression of Keap1 for the wild-type K6a ARE-luciferase reporter plasmid in 293 cells, but mutation of the ARE reversed Nrf2-mediated induction of luciferase (data not shown). These results suggest that Nrf2 may act as a direct transcriptional regulator of certain squamous differentiation genes through their respective AREs.

Induction of phase II detoxifying enzymes

Keap1 represses transcriptional activity of Nrf2 by sequestering it in the cytoplasm[6]. In the present context, we examined whether the expression of Nrf2 target genes is upregulated in the Keap1-deficient mouse. Because *Keap1*$^{-/-}$ mice die within three weeks after birth, we recovered RNA and protein samples from MEFs, from whole embryos at 12.5 d, from neonates and from P10 livers.

We examined the expression of GSTπ and NQO1, two representative phase II enzymes, by RNA-blot hybridization. As expected, both *Gstp1* and *Nqo1* mRNAs were more abundant in the *Keap1*$^{-/-}$ mouse relative to equivalent samples from wild-type or heterozygous mutants (**Fig. 6a**). Whereas the expression of phase II genes is normally inducible only by specific xenobiotics, they are constitutively induced in *Keap1*$^{-/-}$ mice. Consistent with the results of RNA analysis, constitutive expression of both GSTμ and GSTπ was markedly elevated in the P10 *Keap1*$^{-/-}$ liver, regardless of gender (**Fig. 6b**).

Mechanistically, we interpreted these data to suggest that Nrf2 was liberated from its usual cytoplasmic localization in the absence of Keap1, allowing free Nrf2 migration to the nucleus to activate Nrf2 target genes. To test this hypothesis, we examined Nrf2 accumulation in liver nuclear extracts. Immunoblot analysis showed that Nrf2 was significantly more abundant in the nuclei of P10 *Keap1*$^{-/-}$ liver than in wild-type liver (**Fig. 6c**). These results indicate that the phenotypic changes in the *Keap1*-disrupted mouse are largely, if not exclusively, attributable to the high steady-state nuclear accumulation of Nrf2 due to the loss of Keap1.

We previously showed that electrophiles, such as diethylmaleate (DEM), induce Nrf2 target genes[7]. To address whether DEM acts independently of Keap1 or affects the Nrf2-Keap1 interaction, we examined the expression of a group of drug metabolizing and antioxidant enzyme genes by RNA-blot analysis using MEFs from *Keap1*$^{-/-}$, *Nfe2l2*$^{-/-}$, *Keap1*$^{-/-}$ *Nfe2l2*$^{-/-}$ or wild-type embryos. Heavy and light chains of γ-glutamylcysteine synthase (encoded by *Gclc*), NQO1 and peroxiredoxin I (encoded by *Prdx1*) were all induced by DEM in wild-type MEFs (**Fig. 6d**). Notably, these same mRNAs were constitutively induced in Keap1-deficient fibroblasts, but DEM did not further increase the mRNA levels of these enzymes. The constitutive induction of these defense genes was completely abolished when Nrf2 was simultaneously deleted from the *Keap1*$^{-/-}$ mouse (**Fig. 6e**). Similarly, in *Nfe2l2*-null MEFs, *Gclc*, *Nqo1* and *Prdx1* mRNAs were no longer inducible by DEM. These results indicate that Keap1 acts as an indispensable regulator of Nrf2.

Rescue of Keap1 deficiency by loss of Nrf2 function

Our analyses thus far suggested that the growth retardation observed in *Keap1*$^{-/-}$ mice was an indirect consequence of constitutive nuclear accumulation, and thus inappropriate activity, of Nrf2. To ascertain whether Keap1 acts as a direct negative regulator of Nrf2 and whether Nrf2 has a direct role in the *Keap1*-null mutant phenotypes, we examined further compound *Keap1-Nfe2l2* mutant mice. If high-level constitutive expression of Nrf2 is a consequence of *Keap1* mutant phenotypes, reduction of Nrf2 abundance in the *Keap1*-null mutant background should reverse the phenotype and rescue the

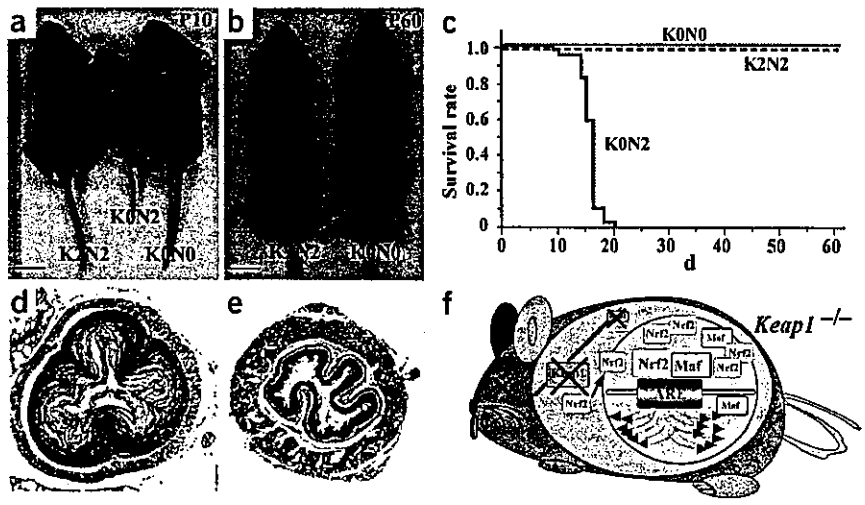

Figure 7 Nrf2 loss rescues Keap1 mutant phenotypes. (**a**) Rescue of *Keap1* mutant mice from lethality by crossing with the germline *Nfe2l2* mutant. Whereas a P10 *Keap1* homozygous mutant mouse (K0N2; middle) showed growth retardation and juvenile death when compared with a wild-type littermate (K2N2), simultaneous mutation of the *Nfe2l2* gene restored their growth (K0N0). (**b**) A *Keap1-Nfe2l2* compound mutant (K0N0) and wild-type littermate at P60 show no obvious phenotypic differences. (**c**) Simultaneous *Nfe2l2* mutation rescues the *Keap1* mutation. Kaplan-Meier survival curves for *Keap1* mutant (red line; $n = 41$), *Keap1-Nfe2l2* compound mutant (green line; $n = 30$) and wild-type (broken line; $n = 25$) mice. (**d**,**e**) The hyperkeratosis and constriction of the homozygous *Keap1* mutant esophagus are rescued in the *Keap1-Nfe2l2* compound mutant. Thin sections of *Keap1* mutant (K0N2, **d**) and *Keap1-Nfe2l2* compound mutant (K0N0, **e**) esophagi are shown after staining with hematoxylin and eosin. (**f**) A model for Keap-Nrf2 complex function *in vivo*. In the wild-type mouse, Keap1 retains Nrf2 in the cytoplasm under normal conditions, and xenobiotic or oxidative stress liberates Nrf2 from Keap1 sequestration, allowing Nrf2 to freely migrate into the nucleus. Nrf2 then activates ARE-mediated transcription of detoxifying and antioxidant enzyme genes. In the absence of Keap1, however, Nrf2 migrates in an unregulated manner to the nucleus, leading to high-level constitutive activation of Nrf2 target gene expression.

Keap1-null mutant mice from lethality. We had previously generated a *Nfe2l2*-null mutant mouse[5], and so we generated compound heterozygous *Keap1*$^{+/-}$ *Nfe2l2*$^{+/-}$ mice and then intercrossed them. In support of the hypothesis that Keap1 function is to sequester Nrf2 in the cytoplasm, all *Keap1*$^{-/-}$ *Nfe2l2*$^{-/-}$ compound mutant mice were healthy and viable for much longer than three weeks after birth (**Fig. 7a,b**). In contrast, all *Keap1*$^{-/-}$ mutants that we recovered from these intercrosses died by P21 (**Fig. 7c**).

The compound homozygous mutant mice were indistinguishable, by size or appearance, from wild-type littermates at P10 or P60 (**Fig. 7a,b**). The scaling skin phenotype of the *Keap1*-null mouse was absent from the compound mutant mice. Histological analysis showed that the hyperkeratotic phenotype of *Keap1*$^{-/-}$ esophagi (**Fig. 7d**) was rescued to normalcy in the compound-null mutant esophagus (**Fig. 7e**). The constitutive overexpression of phase II enzymes and antioxidant proteins that we observed in the *Keap1*-null mutant liver and MEFs also disappeared in the compound mutant mice (**Fig. 6d,e**).

These combined biochemical and genetic data show that insufficient Keap1 affects the normal development of mice by disrupting the nuclear-to-cytoplasmic distribution of Nrf2 (**Fig. 7f**). Because *Nfe2l2* disruption rescues the *Keap1* mutant mouse from pathophysiological hyperkeratosis and growth retardation, we conclude that the Keap1-Nrf2 complex is a vital upstream regulator of a subset of squamous differentiation genes and phase II and antioxidant genes.

DISCUSSION

Nrf2 is a key transcriptional regulatory protein that activates both basal and inducible expression of the phase II and antioxidant enzyme genes[6]. We showed here that Keap1 is an indispensable repressor of Nrf2 function *in vivo*. In mice missing Keap1, Nrf2 accumulates in nuclei at constitutively high levels, leading to the overproduction of cytoprotective enzymes and other cytoprotective proteins. Constitutively activated Nrf2 also affects expression of some of the squamous differentiation genes and causes abnormally thick cornified layers leading to obstruction of the esophagus and cardiac part. Additional disruption of *Nfe2l2* in the *Keap1*-null background reverses the aberrant induction of the cytoprotective enzymes and abnormal cornification and completely rescues *Keap1*$^{-/-}$ mice from lethality. These results indicate that Nrf2-Keap1 collaboration is one of the central regulatory nodes for cellular defense against oxidative and xenobiotic stress.

In Nrf2-mediated regulation of a set of detoxifying and antioxidant enzyme genes, Keap1 acts as a cytoplasmic molecular gatekeeper for Nrf2 (ref. 22). Keap1 binds to both Nrf2 and the actin cytoskeleton to retain Nrf2 in the cytoplasm. This sequestration ensures low basal expression of the cytoprotective enzymes in quiescent cells under normal physiological conditions. When oxidative or xenobiotic stimuli release Nrf2 from Keap1-mediated cytoplasmic entrapment, Nrf2 migrates to the nucleus where it functions as a strong transcriptional activator[23]. Thus, Nrf2-Keap1 regulation of oxidative- and xenobiotic-stress response has identified a new and unique mode of nuclear-cytoplasmic collaboration that is conceptually distinct from that used by NF-κB/I-κB[24]or microtubule-based signal transduction[25].

To examine the contribution of the Nrf2-Keap1 collaboration to regulation of cellular defense at the physiological level, we disrupted *Keap1* and examined the expression of Nrf2 target genes in the *Keap1* mutant mouse. As expected, Nrf2 accumulated more abundantly in the nuclei of *Keap1*-null hepatocytes than in controls. Nrf2 target genes were also expressed at markedly higher levels in the homozygous *Keap1* mutant mice and MEFs than in controls. Thus, without Keap1, Nrf2 migrates freely into the nucleus and constitutively activates the transcription of cytoprotective enzyme genes, even under unstressed conditions (**Fig. 7f**). These results show that Nrf2 and Keap1 cooperate *in vivo* and that this collaboration contributes to the regulation of constitutive and inducible expression of cellular defense genes.

In the *Keap1*-deficient mouse, we observed abnormal keratinization and cornification in the esophagus and forestomach. This unusual accumulation of cornified layers was not observed at the embryonic or P2 stages, indicating that the onset of this abnormal squamous differentiation process occurs after birth. Although the molecular mechanisms leading to the neonatal onset of a specific subset of squamous differentiation genes and hyperkeratosis have not yet been elucidated, the following observations may be pertinent.

First, we found that AREs exist in a subset of genes associated with squamous cell differentiation. Because two of these AREs are functional in transfection assays, and because Nrf2 is expressed in these same epithelial cells, the most straightforward explanation is that Nrf2 binds to these AREs and activates the expression of this set of squamous cell genes *in vivo*. Based on these observations, one can speculate that the Keap1-Nrf2 system may have a role in regulating the response of squamous epithelia to mechanical and environmental stress. The genes encoding keratin K6a and K6b are normally induced in response to stressful stimuli, such as wounding[26]; the hyperkeratotic lesions that develop on the tongues of K6a and K6b double knockout mice during suckling suggest that these keratins may be induced to provide additional structural support in areas that have to withstand increased mechanical stress[27]. Loricrin is a main cell envelope component that confers mechanical stability to cornified tissues. In the absence of loricrin, compensatory mechanisms induce the expression of several known and novel cell envelope components to maintain mechanical integrity[28]. Although the molecular mechanisms regulating this compensatory response have not yet been determined, preliminary evidence suggests that three of the genes upregulated in the loricrin-deficient mice, those encoding SPRRP2D, SPRRP2H and repetin[28], contain AREs and are upregulated in the *Keap1*$^{-/-}$ mutant mouse (Y. Kawachi, M.Y. and D.R.R., unpublished data).

Second, it is known that during desquamation of cornified layers, keratin oxidation is important in increasing the susceptibility of keratins to proteases[29]. As Nrf2 regulates the expression of antioxidant genes[7], constitutive overexpression of Nrf2 in *Keap1* mutant mice may prevent keratins and other differentiation products from oxidation and degradation; this, in turn, may lead to retention of cornified layers in the skin, esophagus and forestomach. When we detected disulfide bonds *in situ* to compare the protein redox states between wild-type and *Keap1*$^{-/-}$ esophagi, the signals in the latter sample were weaker than those in the former (data not shown). This result is expected, indicating that proteins in *Keap1*$^{-/-}$ esophagus are less oxidized. But we detected no decrease in the abundance of oxidized forms of K1 or K10 in *Keap1*-null esophagus (data not shown). Thus, this possibility requires further testing.

The transient scaling phenotype of *Keap1*$^{-/-}$ mouse skin is similar to a human disorder known as autosomal recessive congenital ichthyosis (ARCI; ref. 30). Individuals with ARCI present either lamellar ichthyosis or congenital ichthyosiform erythroderma. Three loci are associated with ARCI. The 14q11 locus has been shown to encode transglutaminase 1 (ref. 31), which catalyzes the formation of the cornified cell envelope. ARCI can also arise from a deficiency at 2q33–35 (ref. 32). A third locus, corresponding to chromosome 19p13.1–13.2, has recently been identified by a genome-wide scan with polymorphic microsatellite markers of samples from five affected

individuals from a Finnish family with ARCI[33]. We found that the human *KEAP1* locus is located at the same chromosomal position as this third ARCI locus, 19p13.1–13.2. Thus, *KEAP1* may have some relationship to ARCI. The scaling of the reported Finnish ARCI cases is mild, similar to the scaling phenotype of the *Keap1* mutants, but the neonatal onset differs from human ARCI.

The genetic rescue of Keap1-deficient mice by the *Nfe2l2* null allele showed that loss of Nrf2 expression rescues *Keap1* mutant mice from lethality. Whereas all *Keap1*-null mutant mice died before three weeks of age, *Keap1-Nfe2l2* compound mutant mice were normal and fertile. The hyperkeratosis phenotype was similarly reversed. Notably, unlike $Keap1^{-/-}$ mice, $Keap1^{-/-}$ $Nfe2l2^{+/-}$ mice survived the crucial postnatal period, but their growth was slower than that of wild-type or $Keap1^{-/-}$ $Nfe2l2^{-/-}$ mice (data not shown). This may indicate that the expression level of cytoprotective enzymes depends on *Nfe2l2* gene dosage in these compound mutant lines, further supporting the contention that the expression of phase II and antioxidant enzyme genes is tightly regulated by the Nrf2-Keap1 pathway.

Our morphological examination strongly suggests that a feeding problem due to hyperkeratotic legions in the esophagus and forestomach is one of the primary causes of the weaning-age lethality. But we cannot exclude the presence of other crucial defects in $Keap1^{-/-}$ pups. Indeed, there may be a large number of Nrf2 target genes, as Nrf2 and Keap1 are both expressed in many tissues. In summary, this study identifies the vital contribution of the Nrf2-Keap1 complex to the regulation of cellular defense mechanisms *in vivo*.

METHODS

Keap1-deficient mice. We isolated two independent clones containing *Keap1* from a 129/SvJ genomic library. To construct targeting vector, we included genes encoding Diphtheria toxin A (*DTA*) and neomycin resistance (neo^r) for negative and positive selection, respectively. We replaced residues 8–204 of Keap1 with both neo^r and NLS-tagged *lacZ* so that the seven N-terminal amino acid residues of Keap1 were linked in frame to NLS-*lacZ* (see **Supplementary Fig. 1** online). The *DTA* gene was provided by M. M. Taketo (Kyoto University) and was inserted 3′ to the short arm for negative selection.

We linearized the targeting vector and electroporated it into E14 ES cells. We recovered ES cell clones from culture with G418 (GIBCO BRL) and screened them by PCR. Primer sequences are available on request. Through PCR analysis of 360 ES cell clones, we identified 17 that carried the homologous recombinant allele. Positive clones were expanded and genotyped by Southern-blot analysis with 5′ (*Eco*RI-*Xba*I) and 3′ (*Eco*RI-*Sac*I) probes located outside the targeting vector. We generated chimeric mice by microinjection of two independent ES cell clones into C57BL/6J mouse blastocysts. We crossed chimeric males with C57BL/6J females. All mice were treated according to the regulations of Standards for Human Care and Use of Laboratory Animals, University of Tsukuba.

***Keap1-Nfe2l2* compound mutant mice.** Because *Nfe2l2*-null mice are viable and fertile[5], we first generated $Keap1^{+/-}$ $Nfe2l2^{+/-}$ mice and then intercrossed them to produce all possible genotypes of compound null mutant mice (determined by PCR). Primer sequences are available on request.

Induction of phase II enzyme and antioxidant genes in MEFs by DEM. We prepared embryonic day 13.5 MEFs by standard procedures[34], plated them at a density of 7.5×10^5 cells per 100-mm dish and then cultured them to subconfluency. We replaced culture medium with fresh medium with or without DEM (100 μM) and collected cells 4.5 h later for RNA analysis.

RNA-blot analysis. We isolated total RNA using ISOGEN (Nippon Gene). We separated each RNA sample (25 μg) by electrophoresis on a formamide-agarose gel and transferred each to a nylon membrane. Keap1 and other probes were hybridized as described previously[5].

Histological and immunohistochemical analysis. We fixed tissue samples in 3.7% buffered formalin and embedded them in paraffin. We stained sections with hematoxylin and eosin for histological examination. For immunohistochemical analysis, we embedded samples with OCT (Sakura Finetechnical) and processed cryosections with antibodies against cytokeratins; antibodies to K1, K6, K13 and K14 were those described previously[35]. We purchased antibodies to loricrin and involucrin from COVANCE and antibody to PCNA from Zymed.

Protein preparation and immunoblotting. We homogenized livers and esophagi in RIPA buffer containing a protease inhibitor cocktail (NEB). We prepared liver nuclear extracts as described[36]. After adding an equal volume of 2× SDS sample buffer[7] (except 10% SDS for the detection of keratins in the esophagus), we boiled the extracts immediately for 5 min. Proteins applied to SDS-PAGE were either stained with Coomassie brilliant blue or transferred to Immobilon PVDF membranes (Millipore). We blocked membranes, treated them with primary antibody and then allowed them to react with the appropriate secondary antibodies conjugated to horseradish peroxidase (Zymed). Immune complexes were visualized with ECL (Amersham). We stained mouse GSTμ and GSTπ subunits with specific rabbit antibodies[5]. Antibodies recognizing nuclear Lamin B (SantaCruz) or β-galactosidase (ICN) were commercially available. We prepared a new antibody to Nrf2 by injecting the mouse Nrf2 recombinant polypeptide corresponding to the N-terminal region into rabbits (to be described elsewhere).

Note: Supplementary information is available on the Nature Genetics website.

ACKNOWLEDGMENTS

We are grateful to O. Nakajima, F. Irie, M. Osaki, S. Kawauchi, X. Pan, S. Masuda, N. Kaneko, H. Ohkawa and R. Kawai for help; K-C. Lim, M. Kobayashi, K. Igarashi, T. O'Connor, T. Hosoya, M. Nose, Y. Kawachi and T. W. Kensler for useful suggestions; and J. D. Hayes and K. Satoh for antibodies. This work was supported by a grant from the US National Institutes of Health (J.D.E.) and grants from the Ministry of Education, Science, Sports and Culture (K.I., H.M. and M.Y.), JST-ERATO (M.Y.), JST-CREST (H.M.) and PROBRAIN (H.M. and S.T.). N.W. was a JSPS-RFTF postdoctoral fellow.

COMPETING INTERESTS STATEMENT

The authors declare that they have no competing financial interests.

Received 19 June; accepted 15 September 2003
Published online at http://www.nature.com/naturegenetics/

1. Motohashi, H., O'Connor, T., Katsuoka, F., Engel, J.D. & Yamamoto, M. Integration and diversity of the regulatory network composed of Maf and CNC families of transcription factors. *Gene* **294**, 1–12 (2002).
2. Moi, P., Chan, K., Asunis, I., Cao, A. & Kan, Y.W. Isolation of NF-E2-related factor 2 (Nrf2), a NF-E2-like basic leucine zipper transcriptional activator that binds to the tandem NF-E2/AP1 repeat of the beta-globin locus control region. *Proc. Natl. Acad. Sci. USA* **91**, 9926–9930 (1994).
3. Itoh, K., Igarashi, K., Hayashi, N., Nishizawa, M. & Yamamoto, M. Cloning and characterization of a novel erythroid cell-derived CNC family transcription factor heterodimerizing with the small Maf family proteins. *Mol. Cell. Biol.* **15**, 4184–4193 (1995).
4. Marini, M.G. *et al.* hMAF, a small human transcription factor that heterodimerizes specifically with Nrf1 and Nrf2. *J. Biol. Chem.* **272**, 16490–16497 (1997).
5. Itoh, K. *et al.* An Nrf2/small Maf heterodimer mediates the induction of phase II detoxifying enzyme genes through antioxidant response elements. *Biochem. Biophys. Res. Commun.* **236**, 313–322 (1997).
6. Itoh, K. *et al.* Keap1 represses nuclear activation of antioxidant responsive elements by Nrf2 through binding to the amino-terminal Neh2 domain. *Genes Dev.* **13**, 76–86 (1999).
7. Ishii, T. *et al.* Transcription factor Nrf2 coordinately regulates a group of oxidative stress-inducible genes in macrophages. *J. Biol. Chem.* **275**, 16023–16029 (2000).
8. Enomoto, A. *et al.* High sensitivity of Nrf2 knockout mice to acetaminophen hepatotoxicity associated with decreased expression of ARE-regulated drug metabolizing enzymes and antioxidant genes. *Toxicol. Sci.* **59**, 169–177 (2001).
9. Ramos-Gomez, M. *et al.* From the Cover: Sensitivity to carcinogenesis is increased and chemoprotective efficacy of enzyme inducers is lost in nrf2 transcription factor-deficient mice. *Proc. Natl. Acad. Sci. USA* **98**, 3410–3415 (2001).
10. Aoki, Y. *et al.* Accelerated DNA adduct formation in the lung of the Nrf2 knockout mouse exposed to diesel exhaust. *Toxicol. Appl. Pharmacol.* **173**, 154–160 (2001).
11. Adams, J., Kelso, R. & Cooley, L. The kelch repeat superfamily of proteins: propellers of cell function. *Trends Cell Biol.* **10**, 17–24 (2000).
12. Oyake, T. *et al.* Bach proteins belong to a novel family of BTB-basic leucine zipper transcription factors that interact with MafK and regulate transcription through the NF-E2 site. *Mol. Cell. Biol.* **16**, 6083–6095 (1996).
13. Yoshida, C. *et al.* Long range interaction of *cis*-DNA elements mediated by architectural transcription factor Bach1. *Genes Cells* **4**, 643–655 (1999).
14. Zipper, L.M. & Mulcahy, R.T. The Keap1 BTB/POZ dimerization function is required

to sequester Nrf2 in cytoplasm. *J. Biol. Chem.* **277**, 36544–36552 (2002).
15. Robinson, D.N. & Cooley, L. *Drosophila* kelch is an oligomeric ring canal actin organizer. *J. Cell Biol.* **138**, 799–810 (1997).
16. Bork, P. & Doolittle, R.F. Drosophila kelch motif is derived from a common enzyme fold. *J. Mol. Biol.* **236**, 1277–1282 (1994).
17. Fulop, V. & Jones, D.T. Beta propellers: structural rigidity and functional diversity. *Curr. Opin. Struct. Biol.* **9**, 715–721 (1999).
18. Xue, F. & Cooley, L. kelch encodes a component of intercellular bridges in *Drosophila* egg chambers. *Cell* **72**, 681–693 (1993).
19. Sinha, S., Degenstein, L., Copenhaver, C. & Fuchs, E. Defining the regulatory factors required for epidermal gene expression. *Mol. Cell. Biol.* **20**, 2543–2555 (2000).
20. DiSepio, D. *et al.* Characterization of loricrin regulation *in vitro* and in transgenic mice. *Differentiation* **64**, 225–235 (1999).
21. Takahashi, K., Yan, B., Yamanishi, K., Imamura, S. & Coulombe, P.A. The two functional keratin 6 genes of mouse are differentially regulated and evolved independently from their human orthologs. *Genomics* **53**, 170–183 (1998).
22. Itoh, K., Ishii, T., Wakabayashi, N. & Yamamoto, M. Regulatory mechanisms of cellular response to oxidative stress. *Free Radic. Res.* **31**, 319–324 (1999).
23. Katoh, Y. *et al.* Two domains of Nrf2 cooperatively bind CBP, a CREB binding protein, and synergistically activate transcription. *Genes Cells* **6**, 857–868 (2001).
24. Li, N. & Karin, M. Signaling pathways leading to nuclear factor-kappa B activation. *Methods Enzymol.* **319**, 273–279 (2000).
25. Robbins, D.J. *et al.* Hedgehog elicits signal transduction by means of a large complex containing the kinesin-related protein costal2. *Cell* **90**, 225–234 (1997).
26. Wojcik, S.M., Bundman, D.S. & Roop, D.R. Delayed wound healing in keratin 6a knockout mice. *Mol. Cell. Biol.* **20**, 5248–5255 (2000).
27. Wojcik, S.M., Longley, M.A. & Roop, D.R. Discovery of a novel murine keratin 6 (K6) isoform explains the absence of hair and nail defects in mice deficient for K6a and K6b. *J. Cell. Biol.* **154**, 619–630 (2001).
28. Koch, P.J. *et al.* Lessons from loricrin-deficient mice: compensatory mechanisms maintaining skin barrier function in the absence of a major cornified envelope protein. *J. Cell. Biol.* **151**, 389–400 (2000).
29. Thiele, J.J., Hsieh, S.N., Briviba, K. & Sies, H. Protein oxidation in human stratum corneum: susceptibility of keratins to oxidation *in vitro* and presence of a keratin oxidation gradient *in vivo*. *J. Invest. Dermatol.* **113**, 335–339 (1999).
30. Williams, M.L. & Elias, P.M. Heterogeneity in autosomal recessive ichthyosis. Clinical and biochemical differentiation of lamellar ichthyosis and nonbullous congenital ichthyosiform erythroderma. *Arch. Dermatol.* **121**, 477–488 (1985).
31. Russell, L.J., DiGiovanna, J.J., Hashem, N., Compton, J.G. & Bale, S.J. Linkage of autosomal recessive lamellar ichthyosis to chromosome 14q. *Am. J. Hum. Genet.* **55**, 1146–1152 (1994).
32. Parmentier, L. *et al.* Mapping of a second locus for lamellar ichthyosis to chromosome 2q33–35. *Hum. Mol. Genet.* **5**, 555–559 (1996).
33. Virolainen, E. *et al.* Assignment of a novel locus for autosomal recessive congenital ichthyosis to chromosome 19p13.1–p13.2. *Am. J. Hum. Genet.* **66**, 1132–1137 (2000).
34. Tiemann, F. & Deppert, W. Immortalization of BALB/c mouse embryo fibroblasts alters SV40 large T-antigen interactions with the tumor suppressor p53 and results in a reduced SV40 transformation-efficiency. *Oncogene* **9**, 1907–1915 (1994).
35. Yuspa, S.H., Kilkenny, A.E., Steinert, P.M. & Roop, D.R. Expression of murine epidermal differentiation markers is tightly regulated by restricted extracellular calcium concentrations *in vitro*. *J. Cell Biol.* **109**, 1207–1217 (1989).
36. Dignam, J.D. Preparation of extracts from higher eukaryotes. *Methods Enzymol.* **182**, 194–203 (1990).